

Original Article

Cite this article: Garza HK, Catlos EJ, Chamberlain KR, Suarez SE, Brookfield ME, Stockli DF, and Batchelor RA (2023) How old is the Ordovician–Silurian boundary at Dob’s Linn, Scotland? Integrating LA-ICP-MS and CA-ID-TIMS U-Pb zircon dates. *Geological Magazine* **160**: 1775–1789. <https://doi.org/10.1017/S0016756823000717>

Received: 14 April 2023

Revised: 28 October 2023

Accepted: 30 October 2023

First published online: 22 November 2023

Keywords:







geochronology; biostratigraphy; LA-ICP-MS; CA-ID-TIMS; U-Pb; Ordovician; Silurian

Corresponding author:

Hector K. Garza;

Email: hector.garza@utexas.edu

How old is the Ordovician–Silurian boundary at Dob’s Linn, Scotland? Integrating LA-ICP-MS and CA-ID-TIMS U-Pb zircon dates

Hector K. Garza^{1,2} , Elizabeth J. Catlos^{1,2} , Kevin R. Chamberlain³,
Stephanie E. Suarez⁴ , Michael E. Brookfield¹ , Daniel F. Stockli¹  and
Richard A. Batchelor⁵ 

¹Jackson School of Geosciences, University of Texas at Austin, Austin, TX, USA; ²Center for Planetary Systems Habitability, University of Texas at Austin, Austin, TX, USA; ³Department of Geology and Geophysics, University of Wyoming, Laramie, WY, USA; ⁴Department of Earth and Atmospheric Sciences, University of Houston, Houston, TX, USA and ⁵School of Geography & Geosciences, University of St. Andrews, St Andrews, Fife, SC, UK

Abstract

Sedimentary rocks exposed at Dob’s Linn, Scotland, have significantly influenced our understanding of how life evolved over the Ordovician to Early Silurian. The current interpreted chronostratigraphic boundary between the Ordovician and Silurian periods is a Global Boundary Stratotype Section and Point (GSSP), calibrated to 443.8 ± 1.5 Ma (Hirnatian–Rhuddanian age), based on biostratigraphic markers, radioisotopic dates and statistical modelling. However, challenges arise due to tectonic disturbances, complex correlation issues and the lack of systematic dating in Ordovician–Silurian stratigraphic sections. Here, hundreds of zircon grains from three metabentonite ash horizons were dated using Laser Ablation Inductively Coupled Plasma Mass Spectrometry (LA-ICP-MS). A subset of the grains were re-analyzed using Chemical Abrasion Isotope Dilution Thermal Ionization Mass Spectrometry (CA-ID-TIMS). We present a high-precision CA-ID-TIMS ^{238}U – ^{206}Pb weighted mean date of $440.44 \pm 0.55/0.56/0.72$ Ma (\pm analytical/with tracer/with U-decay constant) for the *Coronagraptus cyphus* biozone. However, the study reports younger, and in certain cases, older LA-ICP-MS zircon dates within the *Coronagraptus cyphus*, *Akidograptus ascensus* and *Dicellograptus anceps* zones, suspected as being influenced by Pb loss and LA-ICP-MS matrix mismatch. The study reports concerns about the suitability of Dob’s Linn as a GSSP section and examines various LA-ICP-MS maximum depositional age (MDA) approaches, suggesting the use of the TuffZirc date and the youngest mode weighted mean (YMWM) as suitable MDA calculations consistent with CA-ID-TIMS results.

1. Introduction

Evaluating the boundary between the Ordovician–Silurian periods and interpreting the timing and duration of environmental and biological changes requires precise and accurate dating of stratigraphic sections that contain rocks of these time frames. This specific boundary is fundamental to comprehending how life appeared and radiated on this planet as well as understanding the timing of the Late Ordovician Mass Extinction (LOME) (Lenton *et al.* 2012; Wallace *et al.* 2017; Servais *et al.* 2019; Dahl *et al.* 2021). Calibrating relative timescales with isotopic dating of igneous rocks has been an ongoing task since the early days of radiometric dating (Holmes, 1911). Biostratigraphic boundary ages are continually revised with new methods, concepts and studies (Mattinson, 2013; Gradstein & Ogg, 2020). The development of accurate and precise zircon U-Pb dating methods has revolutionised the calibration of many parts of the geologic timescale (Bowring *et al.* 2006; Schoene *et al.* 2013; Spencer *et al.* 2016). The Ordovician and Silurian, however, suffer from a lack of systematic dating of volcanic lavas, breccias and ashes interstratified with biostratigraphically dated sediments. Furthermore, many local biostratigraphic schemes for different areas cannot be accurately correlated between marine and non-marine sections. Thus, the North American, British and Scandinavian schemes suffer from a number of correlation problems, and the Mediterranean and North Gondwanan schemes, and it is complicated to relate to the standard Series and Stages (Sweet & Bergström, 1984; Berry, 1987; Finney, 2005; Fortey, 2011).

Laser Ablation Inductively Coupled Plasma Mass Spectrometry (LA-ICP-MS) and Secondary Ion Mass Spectrometry (SIMS) allow for rapid U-Pb dating of zircons to determine provenance and maximum depositional ages (MDAs) (Table 1). Some studies show that LA-ICP-MS and SIMS methods have systematic biases in ^{238}U – ^{206}Pb zircon dates relative to those obtained using the more precise yet destructive Chemical Abrasion Isotope Dilution

© The Author(s), 2023. Published by Cambridge University Press. This is an Open Access article, distributed under the terms of the Creative Commons Attribution licence (<http://creativecommons.org/licenses/by/4.0/>), which permits unrestricted re-use, distribution and reproduction, provided the original article is properly cited.



Table 1. List of commonly used maximum depositional age (MDA) methods modified from Sharman and Malkowski (2020)

MDA Technique	Abbreviation	Reference
Youngest single grain	YSG	Ludwig and Mundil (2002)
Youngest three grains	Y3Za	Zhang <i>et al.</i> (2016)
Youngest three grains overlapping within uncertainty	Y3Zo	Ross <i>et al.</i> (2017)
Youngest cluster (1 σ overlap)	YC1 σ	Dickinson and Gehrels (2009)
Youngest cluster (2 σ overlap)	YC2 σ	Dickinson and Gehrels (2009)
Youngest statistical population	YSP	Coutts <i>et al.</i> (2019)
Youngest mode kernel density estimation	YMKDE	Herriott <i>et al.</i> (2019)
TuffZirc date	TuffZirc date	Ludwig and Mundil (2002)
Youngest mode weighted mean	YMWM	Tian <i>et al.</i> (2022)

Thermal Ionization Mass Spectrometry method (CA-ID-TIMS) (Mattinson, 2005; Allen & Campbell, 2012; Crowley *et al.* 2014; Marillo-Sialer *et al.* 2014; Von Quadt *et al.* 2014; Watts *et al.*, 2016; Catlos *et al.* 2021). For these reasons, understanding the U-Pb zircon system and potential systematic biases is crucial to produce accurate dates for MDAs of sections of interest.

Here, we report a high-resolution zircon ^{238}U - ^{206}Pb CA-ID-TIMS date for the *Coronagraptus cyphus* biozone and test various LA-ICP-MS MDA calculations to determine suitable MDA approaches for the *Coronagraptus cyphus*, *Akidograptus ascensus* and *Dicellograptus anceps* zones from the tectonically disturbed metabentonites encompassing the Ordovician–Silurian boundary at Dob's Linn, Scotland (Fig. 1). We compare CA-ID-TIMS and LA-ICP-MS zircon U-Pb dates from three graptolite zones showing significantly younger and, in some cases, older LA-ICP-MS zircon dates than anticipated. The discrepancies between CA-ID-TIMS and LA-ICP-MS with the younger and older LA-ICP-MS zircon dates indicate that such dates need careful evaluation and can be variously interpreted as a result of Pb loss, matrix mismatch and/or potential biostratigraphic misplacement, bringing doubt to the validity of Dob's Linn as a Global Boundary Stratotype Section and Point (GSSP) reference section.

2. Geochronology Background

Zircon is a mineral that is resistant to weathering and thus often used to date the MDA of sedimentary sections (Carroll, 1953; Balan *et al.* 2001; Finch & Hanchar, 2003). U-Pb zircon geochronology is considered the optimal radioisotopic dating approach because two decay schemes generate two independent chronometers that can be cross-validated over geologic time. The two independent radioactive decay schemes consist of ^{235}U - ^{207}Pb and ^{238}U - ^{206}Pb , each with a different half-life, permitting identification of inherited domains and open-system behaviour (i.e., Pb loss) (Bowring *et al.* 2006; Corfu, 2013; Schoene, 2014). Three U-Pb dating methods can be used to date lavas and ashes; however, accuracy and precision vary significantly depending on the dating technique (Condon & Bowring, 2011; Spencer *et al.*

2016). As seen in Fig. 2, these approaches sample different portions of the zircon and yield different ranges of precision (Bowring *et al.* 2006; Condon & Bowring, 2011; Spencer *et al.* 2016). LA-ICP-MS is a high-speed and cost-effective dating technique with moderate precision, but depending on preparation methods, such as whether the unknown and standard zircons are annealed or not, can produce 2 σ analytical precision of 1–8% (Von Quadt *et al.* 2014; Schaltegger *et al.* 2015; Ver Hoeve *et al.* 2018). Zircon grains are analyzed with a 10–60 μm spot size and 5–20 μm laser depth at a rate of 20 second–4 minutes per analysis (Bowring *et al.* 2006; Mako *et al.* 2021). SIMS, which includes Sensitive High-Resolution Ion Micro Probe (SHRIMP), is a rapid technique with a 2 σ precision of 1–5%, 10–20 μm spot size, <2 μm analysis depth and a rate of 10–30 minutes per analysis (Bowring *et al.* 2006; Schaltegger *et al.* 2015; Tichomirowa *et al.* 2019). The most precise and accurate technique is Isotope Dilution Thermal Ionization Mass Spectrometry (ID-TIMS), with an additional chemical abrasion (CA-ID-TIMS) option capable of removing radiation-damaged and Pb loss domains in zircon grains. ID-TIMS requires several days of preparation in clean chemistry lab environment and takes 5–6 hours per mass spectrometric analysis with a 2 σ age precision of $\leq 0.3\%$, while CA-ID-TIMS improves the accuracy of the dates by eliminating the effects of Pb loss and produces 2 σ age precisions of $\leq 0.1\%$ (Mattinson, 2005; Bowring *et al.* 2006; Schaltegger *et al.* 2015). Isotope dilution using a well-calibrated isotopic tracer eliminates the dependence on standard measurements and potential matrix mismatches that limit the accuracy and precision of spot analyses (LA-ICP-MS and SIMS; Bowring *et al.* 2006).

Although accuracy and precision from LA-ICP-MS, SIMS and CA-ID-TIMS vary, each of these dating techniques has their advantages and limitations for establishing sedimentary MDAs. CA-ID-TIMS, a time-consuming, costly and destructive technique, functions best with individually dated zircons when accuracy and the highest precision are required. These evaluations pair well with cathodoluminescence (CL) imaging and pre-screening with LA-ICP-MS or SIMS to target the youngest autocrystic grain population from a temporally distinct magmatic pulse and prevent the inclusion of antecrysts formed from an earlier magma pulse, or xenocrysts included from older host rock during younger magmatic pulses (Rossignol *et al.* 2019; Zellmer, 2021). Additionally, the number of zircon grains per sample from the youngest age mode is significant as there is no assurance that these grains will endure the destructive chemical abrasion process and fully dissolve altogether with the radiation damaged Pb loss zones. Rapid, cost-effective analytical techniques such as LA-ICP-MS and SIMS using laser-coupled plasma or ion bombardment possess a high spatial resolution ideal to target specific domains in samples with abundant quantities of zircon grains. Zircon grains are polished and CL imaged to avoid inherited cores or potential metamict zones. Alternatively, zircons can be depth profiled, providing core-rim spatial information and spread in uranium concentrations. Since zircons are not polished and no CL images are acquired, the depth profile method is not optimal for complex grains with abundant growth zone history (Marsh & Stockli, 2015; Rasmussen *et al.* 2019). However, systematic biases with LA-ICP-MS and SIMS, such as Pb loss and the matrix effect between unknown and standards, are suggested to be the driving mechanism producing discrepancies across dating techniques (Bowring & Schmitz, 2003; Andersen *et al.* 2019).

In the last decade, LA-ICP-MS studies indicate systematic biases with ^{238}U - ^{206}Pb zircon dates relative to CA-ID-TIMS and

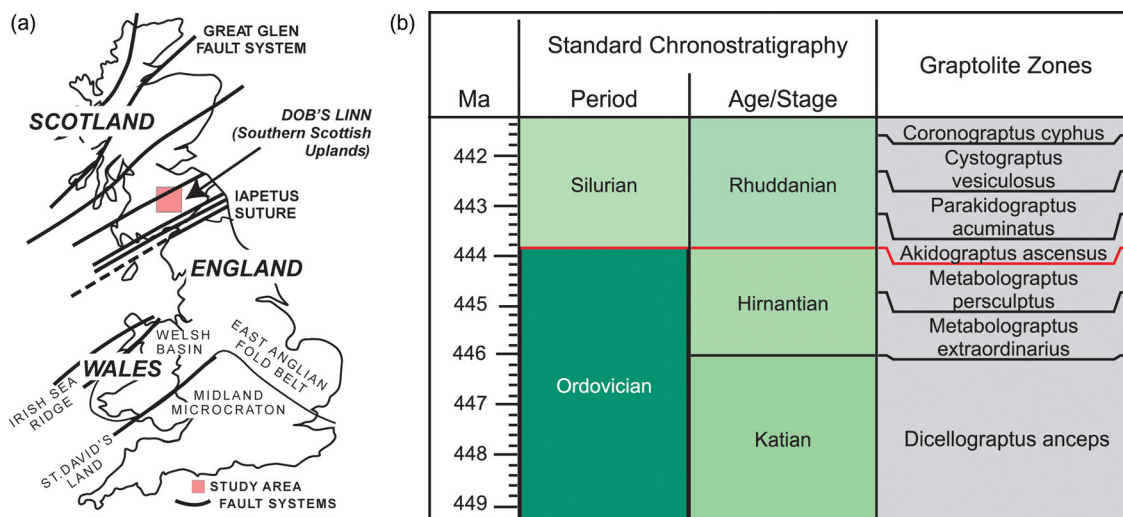


Figure 1. (Colour online) (a) Generalized map of the United Kingdom showing Dob’s Linn study area (red) in the Southern Scottish Uplands. (b) Geological timescale with respective graptolite zones. The red line presents the base of the *Akidograptus ascensus* biozone representing the Ordovician–Silurian boundary.

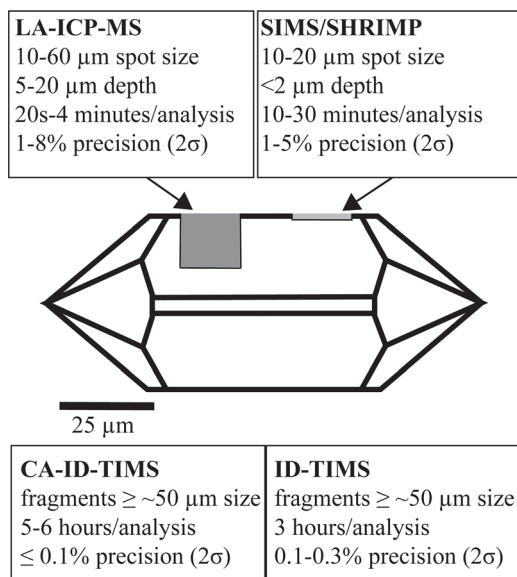


Figure 2. (Colour online) Generalized comparison of zircon U–Pb dating methods. Modified from Bowring *et al.* (2006).

within the LA-ICP-MS technique itself, varying between laboratories. Different laboratories present consistently young or older dates for the identical sample using the same calibration standards as a result of the matrix effect (Marillo-Sialer *et al.* 2014). Matrix mismatch is a recognized systematic bias with LA-ICP-MS U–Pb zircon geochronology that is yet to be entirely comprehended. The three primary factors associated with the matrix effect originate with the zircon grains (unknowns), zircon standards and mass spectrometer ablation conditions (Jackson *et al.* 2004; Allen & Campbell, 2012; Marillo-Sialer *et al.* 2014). It is difficult to obtain identical behaviour between unknown and standard zircons for various reasons, including differences in grain sizes, radiation damage (alpha dose) and maintaining equal laser beam conditions, including spot size, focus, ablation rates and integration time (Jackson *et al.* 2004). Von Quadt *et al.* (2014) suggest that the physical condition of the unknown zircon grains and the utilized standards are the underlying cause of downhole fractionation of Pb

from U, resulting in the matrix effect. According to Marillo-Sialer *et al.* (2014), the primary limitation of LA-ICP-MS is the requirement of the same behaviour between standards and unknowns during analysis. Allen and Campbell (2012) propose that the mechanism driving the matrix effect is the difference between the alpha dose between unknown and standard zircons, thus generating LA-ICP-MS ²³⁸U–²⁰⁶Pb zircon dates younger or older relative to ID-TIMS due to fractionation.

Additionally, factors such as tectonics and hydrothermal alteration can increase radiation damage accumulation experienced by zircon grains, consequently producing metamict Pb loss domains on a case-by-case basis depending on the geologic history and location of the unknown zircon grains (Schoene, 2014). Because radiation damage in zircon grains can vary extensively, it is challenging to utilize a well-characterized zircon standard identical to any possible unknown zircon grains (Jackson *et al.* 2004). However, the concerns of matrix mismatch induced by zircons affected by alpha decay radiation damage domains and spontaneous fission in the crystal lattice can be minimized by annealing both zircon standards and unknowns prior to spot analysis (Allen & Campbell, 2012; Solari *et al.* 2015; Ver Hoeve *et al.* 2018). For example, the well-characterized zircon standards GJ-1 and Plesovice contain metamict sectors that if annealed can improve LA-ICP-MS accuracy and precision (Jackson *et al.* 2004; Sláma *et al.*, 2008; Frei & Gerdes, 2009). According to Ver Hoeve *et al.* (2018), LA-ICP-MS downhole fractionation is one of the principal setbacks in optimizing both precision and accuracy. While thermally annealing unknown grains improves accuracy, if the standards are also annealed then precision can be improved by minimizing downhole fractionation and matrix mismatch by obtaining as close as possible identical behaviour between unknown and standard zircons (Ver Hoeve *et al.* 2018).

3. Geological Background

The Dob’s Linn locality is one of several tectonically disturbed sections of the Moffat Shale Group of Southern Scotland with many intricate minor- and large-scale faults, isoclinal folding, and unresolvable thinning and thickening of strata (Williams, 1988). As shown in Fig. 3, the Dob’s Linn Ordovician–Silurian boundary

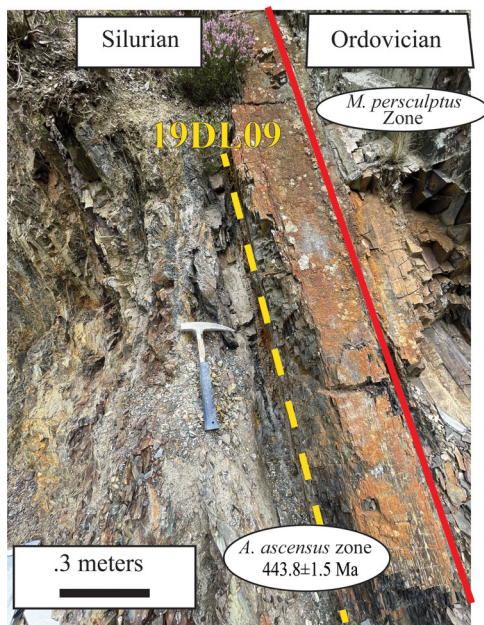


Figure 3. (Colour online) Moffat Shale (Birkhill Shale member) at Dob's Linn's GSSP Linn trench outcrop showing vertical stratigraphy, graptolite horizons and metabentonite horizons that are deformed as a result of extensive tectonic activity. The red line displays the Ordovician–Silurian boundary with an accepted age of 443.8 ± 1.5 Ma (Cohen *et al.* 2013; Cohen *et al.* 2022). The orange dashed line shows sample 19DL09 in the study, a metabentonite horizon in the *Akidograptus ascensus* zone.

GSSP outcrop's bedding is positioned in a vertical direction due to the severe tectonism in southern Scotland. The widespread tectonic activity is associated with the forming of the Caledonian mountains that started during the Early Ordovician (475 Ma) and fully formed by the Late Silurian (425 Ma) (Fig. 4) (Chew & Strachan, 2014). The Moffat shale consists of a pelagic mudrock succession deposited in oceanic, forearc or back-arc environments in Late Ordovician to Early Silurian times (Fig. 4) (Morris, 1987; Stone *et al.* 1987; Merriman & Roberts, 1990).

The Upper Ordovician–Lower Silurian sediments consist of the 48-metres-thick Hartfell Shale Formation subdivided into the Lower and Upper units containing scarce metabentonite horizons. The Lower Hartfell Shale is composed of primarily black mudstone coarsening upwards to cherty and silty mudstone. The Upper Hartfell Shale is characterized by laminated and bioturbated grey mudstone (Williams, 1983; Batchelor & Weir, 1988). The Birkhill Shale Formation is 45 metres thick and likewise sectioned into lower and upper units, with continuous metabentonite successions and a sharp contact between the units. The Lower Birkhill Shale is a black mudstone transitioning to brittle cherty mudstone and with blocky morphology. The Upper Birkhill Shale is a black mudstone transitioning to grey-green mudstone (Batchelor & Weir, 1988; Merriman & Roberts, 1990).

Dob's Linn is considered by some as a significant location due to the appearance of critical graptolite transitions during the Ordovician (485.4–443.8 Ma) and Silurian (443.8–419.2 Ma) periods in the Moffat Shale Group (Fig. 3) (Cocks, 1985, 1988; Williams, 1988; Gradstein *et al.* 2020). This chronostratigraphic boundary was first dated based on biostratigraphic distributions of graptolites (Fig. 1b) (Carruthers, 1858; Nicholson, 1867; Lapworth, 1878). These small, aquatic colonial animals are “unrivaled in the Early Palaeozoic” in terms of subdividing relative time (Zalasiewicz, 2001: 240) and thus are widely used to

correlate sedimentary sections that contain them regionally and globally (Koren' & Rickards, 1979; Williams, 1983). However, the use of correlating these early organisms has been problematic due to local evolutionary provincialism and convoluted age interpretations with the correlation of fluvial and marine deposits with a standard geologic timescale (Berry, 1987; Finney & Chen, 1990; Pogson, 2009; Brookfield *et al.* 2021). Additionally, the Ordovician–Silurian boundary age at Dob's Linn has been estimated by several radioisotopic dates with varying precisions, calculated by spline fitting interpolation from units stratigraphically above and below the boundary (Tucker *et al.* 1990; Hu *et al.* 2008; Schmitz & Ogg, 2020).

4. Biozone ages

4.a. *Coronagraptus cyphus* Biozone

The *Coronagraptus cyphus* biozone located in the Lower Birkhill Shale Formation constrains the end of the Early Silurian Rhuddanian Stage (Fig. 1b) (Ross *et al.* 1982; Tucker *et al.* 1990; Gradstein *et al.* 2020). A zircon fission-track date of 437 ± 10 Ma was initially reported for the *Coronagraptus cyphus* zone in Dob's Linn (Ross *et al.* 1982). Elsewhere, hornblende from the *Coronagraptus cyphus* zone in the Descan Formation in Esquibel Island, Alaska, produced a ^{40}Ar – ^{39}Ar date of 442.6 ± 5.0 Ma (Lanphere *et al.* 1977; Ross *et al.* 1982; Kunk *et al.* 1985; Schmitz & Ogg, 2012). Utilizing mechanically (air) abraded zircon ^{238}U – ^{206}Pb ID-TIMS dates, Tucker *et al.* (1990) produced a biozone age of 439.57 ± 1.33 Ma from the weighted mean of six multigrain zircon fractions from Dob's Linn, Scotland (Table 2) (Schmitz & Ogg, 2020).

4.b. *Akidograptus ascensus* Biozone

The *Akidograptus ascensus* biozone located in the Lower Birkhill Shale Formation has been interpreted to define the Ordovician–Silurian boundary at Dob's Linn, Scotland (Fig. 1b) (Rong *et al.* 2008; Gradstein *et al.* 2020). The *Akidograptus ascensus* zone is dated using various data points including graptolites and stratigraphically upper and lower zircon ID-TIMS U–Pb dates with spline fitting interpolation generating random replications with the input data and validated with a smoothing factor value producing a straight-line fit (Agerberg *et al.* 2020). However, the current age interpretations of 443.8 ± 1.5 Ma or 443.1 ± 0.9 Ma are calculated by spline fitting interpolation from U–Pb multigrain zircon fractions stratigraphically above (*Coronagraptus cyphus* zone) and below (*Dicellograptus anceps* zone) the *Akidograptus ascensus* zone. Gradstein *et al.* (2020) interpolated the Ordovician–Silurian boundary age to 443.1 ± 0.9 Ma from Katian and Rhuddanian ID-TIMS ^{238}U – ^{206}Pb zircon dates from Dob's Linn and a Hirnantian SHRIMP ^{238}U – ^{206}Pb date from South China (Tucker *et al.* 1990; Hu *et al.* 2008; Ogg *et al.* 2016; Schmitz & Ogg, 2020). The International Commission of Stratigraphy interpolated the age of the boundary to 443.8 ± 1.5 Ma only using Dob's Linn's Katian and Rhuddanian ID-TIMS ^{238}U – ^{206}Pb zircon dates (Table 2) (Tucker *et al.* 1990; Cohen *et al.* 2022).

4.c. *Dicellograptus anceps* Biozone

The *Dicellograptus anceps* biozone located in the Upper Hartfell Shale Formation constrains the end of the Late Ordovician Katian Stage (Fig. 1b) (Merriman & Roberts, 1990; Gradstein *et al.* 2020). A zircon fission-track date of 434 ± 12 Ma was first reported

Table 2. Compilation of radioisotopic dates and statistical approaches from previous studies that estimate the ages for graptolite biozones at or near the Ordovician–Silurian boundary

Biozone	Interpreted age (Ma)	Dating technique	Sample locality	References
<i>Dicellograptus anceps</i>	434 ± 12	Zircon Fission track	Dob's Linn, Scotland	Ross (1984)
<i>Dicellograptus anceps</i>	445.7 ± 2.4	Zircon U-Pb TIMS	Dob's Linn, Scotland	Tucker <i>et al.</i> (1990)
<i>Dicellograptus anceps</i>	444.88 ± 1.17	Zircon U-Pb TIMS	Dob's Linn, Scotland	Schmitz & Ogg (2012), Gradstein <i>et al.</i> (2012)
<i>Dicellograptus anceps</i>	4443.81 ± 0.24	Zircon U-Pb TIMS	Wanhe, China	Ling <i>et al.</i> (2019)
<i>Dicellograptus anceps</i>	444.06 ± 0.20	Zircon U-Pb TIMS	Wanhe, China	Ling <i>et al.</i> (2019)
<i>Akidograptus ascensus</i>	443.8 ± 1.5	Spline interpolation	Scotland, China	Gradstein <i>et al.</i> (2012), Cohen <i>et al.</i> (2022)
<i>Akidograptus ascensus</i>	443.1 ± 0.9	Spline interpolation	Scotland, China	Gradstein <i>et al.</i> (2012), Gradstein <i>et al.</i> (2020)
<i>Coronagraptus cyphus</i>	437 ± 10	Zircon Fission track	Dob's Linn, Scotland	Ross <i>et al.</i> (1982)
<i>Coronagraptus cyphus</i>	442.6 ± 5.0	Ar-Ar	Esquibel Island, USA	Lanphere <i>et al.</i> (1977), Kunk <i>et al.</i> (1985)
<i>Coronagraptus cyphus</i>	439.57 ± 1.33	Zircon U-Pb TIMS	Dob's Linn, Scotland	Tucker <i>et al.</i> (1990)

References 1. Ross (1984) 2. Tucker *et al.* (1990); 3. Schmitz & Ogg (2012); 4. Gradstein *et al.* (2012); 5. Ling *et al.* (2019); 6. Cohen *et al.* (2022); 7. Gradstein *et al.* (2020); 8. Ross (Ross *et al.* 1982); 9. Lanphere *et al.* (1977); 10. Kunk *et al.* (1985).

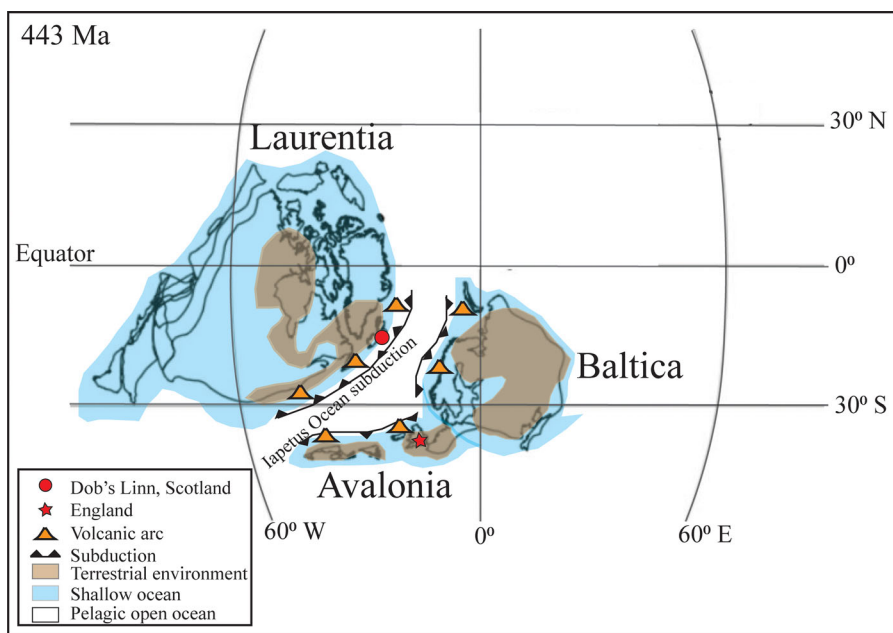


Figure 4. (Colour online) Paleogeographic reconstruction during the Late Ordovician (443 Ma). Closing of the Iapetus Ocean forming volcanic arcs (fore-arc and back-arc) near subduction margins of Laurentia, Baltica and Avalonia, producing widespread tectonic activity and forming the Caledonian mountains (after Huff *et al.* 2010; Chew & Strachan, 2014).

for the *Dicellograptus anceps* zone in Dob's Linn (Ross, 1984). Subsequently, three (of four) multigrain zircon fractions ($n = 58$ of 73 grains analyzed) zircons fractions from the *Dicellograptus anceps* zone, located 4.5 metres below the Ordovician–Silurian boundary, yielded a mechanically (air) abraded zircon ^{238}U - ^{206}Pb ID-TIMS date of 445.7 ± 2.4 Ma (Tucker *et al.* 1990). Using Tucker *et al.* (1990) zircon multigrain fractions and via spline fitting modelling, Schmitz & Ogg (2020) recalculated the age of the biozone to 444.88 ± 1.17 Ma (Schmitz & Ogg, 2020). Elsewhere, the *Metabolograptus extraordinarius* zone in Wanhe, SW China, the equivalent of the *Dicellograptus anceps* zone at Dob's Linn, produced two CA-ID-TIMS ^{238}U - ^{206}Pb dates of 443.81 ± 0.24 Ma and 444.06 ± 0.20 Ma (Table 2) (Ling *et al.* 2019).

5. Methods

In this study, we dated three metabentonite ash horizon samples (DL7, 19DL09 and BRS23) located within the *Dicellograptus anceps*, *Akidograptus ascensus* and *Coronagraptus cyphus* biozones from the Dob's Linn biostratigraphy sections. Dob's Linn is a Site of Special Scientific Interest (SSSI) in Scotland with restrictions on sample collection; thus, sample DL7 from the Main cliff section was provided by Richard Batchelor from archived material (Batchelor & Weir, 1988). Sample BRS23 from the Linn branch trench was provided by the British Geological Survey (Merriman & Roberts, 1990). Sample 19DL09 was collected by Catlos & Brookfield from the Linn branch trench, the same DL9 layer as in Batchelor and Weir (1988) and BRS292 in Merriman and

Roberts (1990). The appropriate authorities granted permission for sample collection.

Traditional heavy mineral separation techniques were used, including deflocculation and extraction of clays via the addition of sodium hexametaphosphate and sonication to obtain maximum zircon yield. Overall, a total of 324 zircon grains were mounted in epoxy and inspected with CL using a JEOL Scanning Electron Microscope at the University of Texas at Austin, GeoMaterials Characterization and Imaging facility (GeoMatCI). Following imaging, zircons were dated using Element2 High Resolution (HR)-LA-ICP-MS in the Geo-thermochronology lab at the University of Texas at Austin. The instrument uses an Excimer (192 nm) laser ablation system and obtains isotopic measurements using ion counting. A dry ablated aerosol is introduced to the instrument by a pure He carrier gas containing the desired isotopic analytes, which for this study consist of ^{238}U , ^{235}U , ^{232}Th , ^{206}Pb , ^{207}Pb and ^{208}Pb . Each analysis consisted of a 2-pulse cleaning ablation, a background measurement taken with the laser off, a 30-second measurement with the laser firing and a 30 second cleaning cycle. The laser beam was 15 μm in diameter to limit analyses to specific CL domains within the zircon crystals and allow for multiple spots per grain in some cases. Elemental isotopic fractionation of Pb and Pb/U isotopes was corrected by interspersed analyses of primary and secondary zircon standards with known ages (GJ1 and Plesovice references) (Jackson *et al.* 2004; Sláma *et al.* 2008). The typical ratio of unknown standards measurements was 3:1 or 4:1. Systematic uncertainties resulting from calibration corrections are usually 1–2% for $^{206}\text{Pb}/^{207}\text{Pb}$ and $^{206}\text{Pb}/^{238}\text{U}$. Pb values are reported as total Pb without any correction for potential common ^{204}Pb due to isobaric interferences with ^{204}Hg . Iolite software was used to process and reduce data analyses, correct instrument drift, and downhole fractionation (<https://iolite-software.com/>).

After LA-ICP-MS analysis, subsets of zircons from samples 19DL09 and BRS23 were removed from epoxy and subjected to CA-ID-TIMS analyses in the geochronology lab at the University of Wyoming adapted from the method of Mattinson (2005). Zircons chosen for this treatment included some of the youngest grains in BRS23 to test whether these dates reflected Pb loss and some of the oldest grains in 19DL09 to test whether these dates reflected matrix mismatch. In the CA process, zircon grains were annealed for 50 hours at 850 °C to repair fission tracks and other minor radiation damage. Zircons were then chemically abraded with HF and HNO₃ acids for 12 hours at 180 °C to partially dissolve and remove metamict portions of the grain that have experienced Pb loss due to substantial radiation damage. Single zircon grains were then spiked with a mixed $^{205}\text{Pb}/^{233}\text{U}/^{235}\text{U}$ EARTHTIME tracer solution (ET535), dissolved in HF and HNO₃ at 235 °C for 30 hours, and converted to chlorides at 180 °C for 16 hours. Dissolved zircon samples were loaded onto single rhenium filaments with silica gel and H₃PO₄ without any further chemical processing except for three larger grains from which the Pb and U were purified on HCl-H₂O ion exchange column following Krogh (1973). Isotopic compositions were measured on a Micromass Sector 54 mass spectrometer in single collector, peak switching mode using the Daly photomultiplier collector for all isotopes (Anderson *et al.* 2013; Barnes *et al.* 2021).

Statistical values and figures, including Concordia diagrams, Kernel density estimates, Tuffzirc dates, and weighted mean distribution plots, were produced by Isoplot, Densityplotter and detritalPy (Ludwig & Mundil, 2002; Ludwig, 2008; Vermeesch, 2012; Sharman *et al.* 2018). A $^{206}\text{Pb}/^{238}\text{U}$ vs $^{207}\text{Pb}/^{235}\text{U}$ 10%

discordance filter was implemented for all LA-ICP-MS zircon dates. Robust CA-ID-TIMS WM dates are calculated from a cluster of four or more of the youngest zircon dates overlapping within uncertainty. The youngest single grain (YSG) MDA approach is calculated from the youngest zircon date (Ludwig & Mundil, 2002). The weighted mean date (WM) is calculated from all individual zircon dates per sample using Isoplot (Ludwig, 2008). TuffZirc date is calculated using Ludwig and Mundil (2002)'s algorithm calculating the median U-Pb date of the largest coherent group of zircons dates with 2σ uncertainty using Isoplot (Ludwig, 2008). The youngest cluster of 2+ grains (YC2 σ +2) is calculated from the weighted mean of the youngest zircon grain cluster of two or more grains overlapping at 2σ uncertainty (Dickinson & Gehrels, 2009). The youngest mode kernel density estimate (YMKDE) (also recognized as YPP by Dickinson and Gehrels (2009) is calculated using Vermeesch (2012)'s Densityplotter from the youngest age peak on a kernel density estimate plot (bandwidth of 10) designed from various U-Pb zircon dates while omitting single grain age peaks (Herriott *et al.* 2019). The youngest statistical population (YSP) is the weighted mean of the youngest subsample of two or more grains that produce a mean square weighted deviation (MSWD) close to 1 (Coutts *et al.* 2019). The youngest mode weighted mean (YMWM) is calculated after Tian *et al.* (2022), using the LA-ICP-MS zircon dates that comprise the youngest age mode from a KDE peak as a weighted mean of more than three grain overlapping at 2σ uncertainty with an approximate MSWD of 1. The KDE peak age serves as the initial reference point, with individual zircon dates extracted from both sides of the crest to attain an MSWD of 1 or an approximate value (Tian *et al.* 2022). The Maximum Likelihood Age (MLA) is computed via a regression algorithm employing error correlations and analytical uncertainties, assuming that data scatter primarily arises from analytical uncertainties. In the case of a correct assumption, the MSWD value should approach one (Vermeesch, 2018, 2021).

6. Results

6.a. *Coronagraptus cyphus* Biozone (Sample BRS23)

Samples BRS23 of the *Coronagraptus cyphus* zone yielded 137 zircon grains analyzed by U-Pb LA-ICP-MS and subset of 15 single grains by CA-ID-TIMS (Fig. 1b). After applying a $\leq 10\%$ discordance filter, 133 grains ranging from Ordovician to Devonian in age were utilized to constrain an MDA for the biozone with various methods to constrain depositional ages. The youngest estimate using U-Pb LA-ICP-MS for sample BRS23 is the YSG date of 392 ± 10 Ma (5% disc), whereas the YC2 σ +2 yields a date of 397 ± 10 ($n = 4$, MSWD = 1.40). The WM presents a date of 439 ± 2 Ma ($n = 133$, MSWD = 5.60), the YMKDE yields a 441 Ma date and the TuffZirc date is $441+2/-3$ Ma ($n = 133$). The MLA produces a date of 440 ± 2 Ma ($n = 133$, MSWD = 5.40), and both the YSP and YMWM date is 440 ± 1 Ma ($n = 83$, MSWD = 1.00). CA-ID-TIMS analyses from the youngest zircon grains yielded a ^{238}U - ^{206}Pb weighted mean age of $440.44 \pm 0.55/0.56/0.72$ Ma (\pm analytical/with tracer/with U-decay constant), (95% conf., MSWD 0.26, 4 of 15 analyses) (Fig. 5a; supplementary tables S1, S2).

6.b. *Akidograptus ascensus* Biozone (Sample 19DL09)

Sample 19DL09 of the *Akidograptus ascensus* zone yielded a total of 19 zircon grains analyzed by U-Pb LA-ICP-MS and subset of single grains by CA-ID-TIMS (Fig. 1b). After applying a $\leq 10\%$

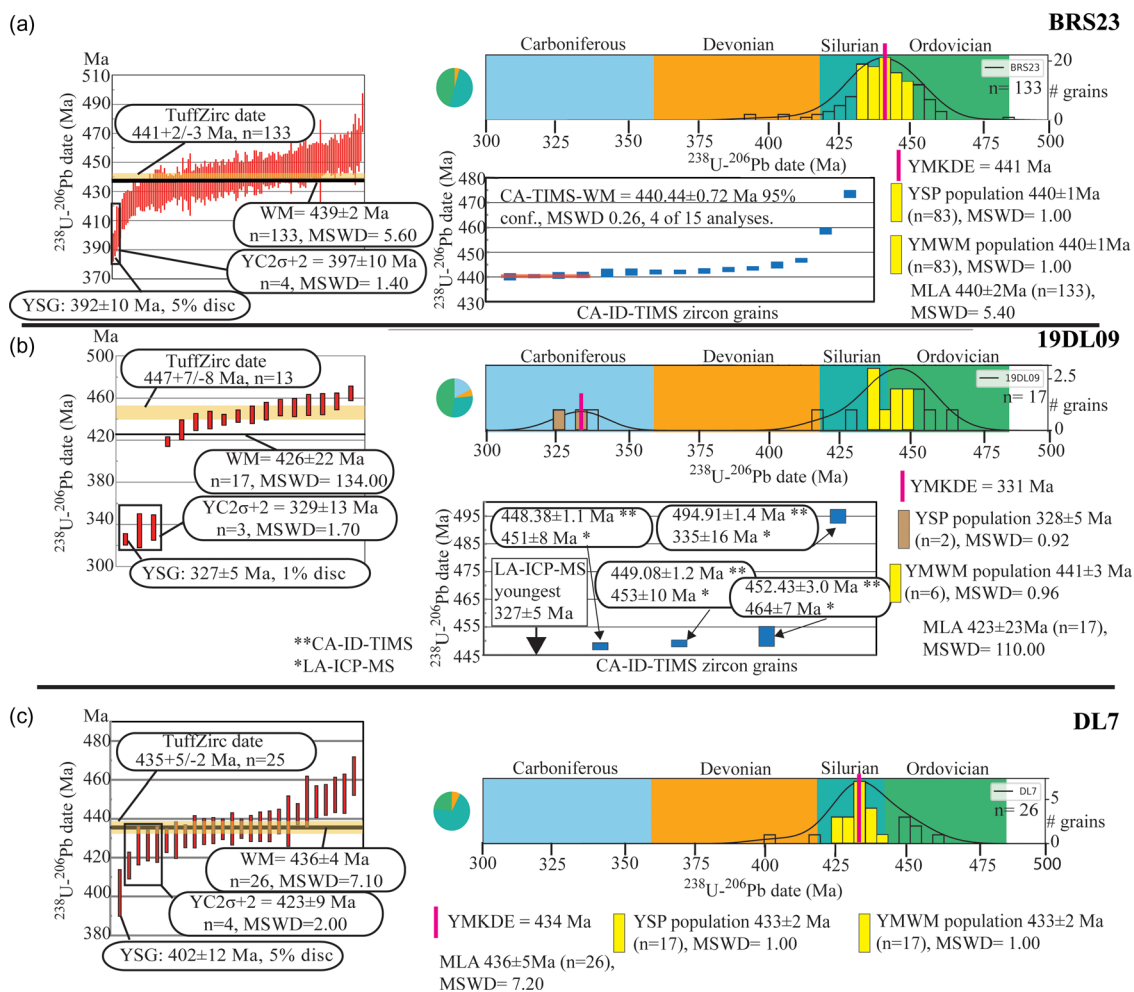


Figure 5. (Colour online) Individual sample ^{238}U - ^{206}Pb LA-ICP-MS dates MDA approach results: youngest single grain (YSG) (Ludwig & Mundil, 2002); youngest cluster 2+ grains at 2σ overlap (YC 2σ +2) (Dickinson & Gehrels, 2009); LA-ICP-MS total weighted mean (WM; black line); TuffZirc date (beige line) (Ludwig & Mundil, 2002); Maximum Likelihood Age (MLA) (Vermeesch, 2021); youngest mode kernel density estimate (YMKDE: pink line) (Herriott *et al.* 2019); youngest statistical population (YSP: yellow or brown bars when applicable) (Coutts *et al.* 2019); youngest mode weighted mean (YMW: yellow bar) (Tian *et al.* 2022) compared to ^{238}U - ^{206}Pb CA-ID-TIMS weighted mean date. (a) Sample BRS23: *Coronagraptus cyphus* zone. (b) Sample 19DL09: *Akidograptus ascensus* zone. (c) Sample DL7: *Dicellograptus anceps* zone.

discordance filter, 17 zircon grains ranging from Ordovician to Middle Carboniferous age are utilized to constrain an MDA for the biozone with several methods to constrain depositional ages. The youngest estimate using U-Pb LA-ICP-MS for sample 19DL09 is the YSG date of 327 ± 5 Ma (1% disc), whereas the YC2 σ +2 yields a date of 329 ± 13 (n = 3, MSWD = 1.70). The WM presents a date of 426 ± 22 Ma (n = 17, MSWD = 134.00), the YMKDE yields a 331 Ma date and the TuffZirc date is $447 \pm 7/-8$ Ma (n = 13). The MLA produces a date of 423 ± 23 Ma (n = 17, MSWD = 110.00), and the YSP produced a date of 328 ± 5 (n = 2, MSWD = 0.92) in addition to a YMW date of 441 ± 3 (n = 6, MSWD = 0.96). An ID-TIMS analysis without chemical abrasion from one of the youngest LA-ICP-MS dated zircon grains yielded a ^{238}U - ^{206}Pb date of 339.64 ± 0.62 Ma. CA-ID-TIMS analyses produced four individual ^{238}U - ^{206}Pb zircon dates from one young grain and three older plateau population grains (older recurring dates overlapping with 2σ uncertainty) previously dated by LA-ICP-MS yielding ^{238}U - ^{206}Pb CA-ID-TIMS dates of 448.38 ± 1.10 Ma, 449.08 ± 1.20 Ma, 452.43 ± 3.00 Ma and 494.91 ± 1.40 Ma (Fig. 5b; supplementary tables S1, S2).

6.c. *Dicellograptus anceps* Biozone (Sample DL7)

Sample DL7 of the *Dicellograptus anceps* zone yielded a total of 40 zircon grains only analyzed by U-Pb LA-ICP-MS. After applying a $\leq 10\%$ discordance filter, 26 grains out of 40 ranging from Ordovician to Devonian age were utilized to constrain an MDA for the biozone (Fig. 5c; supplementary table S1). The youngest estimate using U-Pb LA-ICP-MS for sample DL7 is the YSG date of 402 ± 12 Ma (5% disc), whereas the YC2 σ +2 yields a date of 423 ± 9 (n = 4, MSWD = 2.00). The WM presents a date of 436 ± 4 Ma (n = 26, MSWD = 7.10), the YMKDE yields a 434 Ma date and the TuffZirc date is $435 \pm 5/-2$ Ma (n = 25). The MLA produces a date of 436 ± 5 Ma (n = 26, MSWD = 7.20). Both the YSP and YMW produce a date of 433 ± 2 Ma (n = 17, MSWD = 1.00) (Fig. 5c).

7. Discussion

This study aims to re-assess the current interpretation of Dob's Linn as the 'GSSP' due to the implications of understanding

biological, climatic and environmental events during the Early Paleozoic. Additionally, our study is a benchmark to assess appropriate dating approaches to generate accurate MDAs of Early Paleozoic sections previously calibrated with multi-grain, ID-TIMS zircon U-Pb dates (Tucker *et al.* 1990; Schmitz & Ogg, 2012; Ogg *et al.* 2016; Gradstein *et al.* 2020; Cohen *et al.* 2022). Our study incorporates the preliminary screening of single zircon grains with CL imaging and LA-ICP-MS analyses to target the youngest and plateau populations of volcanic grains with single-grain CA-ID-TIMS analyses. This procedure permits the analysis of autocryst grain populations and filters antecrystic and/or xenocrystic zircon while mitigating the effects of Pb loss.

Concerns remain over the selection of Dob's Linn as the global Ordovician–Silurian boundary stratotype section. According to previous studies, Dob's Linn does not meet the international standards for a GSSP as a result of a complex tectonic and thermal history of the area affecting the stratigraphic position and accuracy of graptolite zone distributions biasing geochronology and chemostratigraphic analyses (Berry, 1987; Lesperance *et al.* 1987; Williams, 1988). The ICS requires a geologic section to fulfill a set of criteria to be considered a GSSP. A GSSP boundary is required to be research accessible and free to access in addition to being extensive enough to allow continuous sample collection for domestic and international researchers. A GSSP must contain a stratigraphic marker that defines the lower boundary of a geologic Stage. The boundary must present diversity and abundance of well-preserved fossils throughout the boundary interval, including secondary markers such as other fossils and chemical changes manifested in regional and global stratigraphic sections. The stratigraphic section must have layers containing minerals that can be radiometrically dated and adequate thickness allowing global correlation, including continuous sedimentation without gaps or changes in facies. The boundary is required to be unaffected by tectonic disturbances and metamorphism (Remane *et al.* 1996; Gradstein & Ogg, 2020).

Initially, Dob's Linn was selected in 1979 by the Boundary Working Group as the GSSP for the base of the *Parakidograptus acuminatus* zone marking the base of the Silurian and thus the Ordovician–Silurian boundary and later reassessed to the *Akidograptus ascensus* graptolite zone (Fig. 1b) (Ross, 1984; Cocks, 1985, 1988; Rong *et al.* 2008). The primary concerns for questioning Dob's Linn as a reference section is due to the limited lateral extent of graptolite zones, scarcity of fossils other than graptolites, and the locality's tectonic and thermal disturbed sections forming large and micro-scale folds and faults across the Moffat Shale, disputing the accuracy of the graptolite data (Leggett *et al.* 1979; Williams, 1983; Williams & Rickards, 1984; Berry, 1987; Lesperance *et al.* 1987; Williams, 1988). Isotopic carbon data points to the *Metabolograptus persculptus* zone as a possibility this graptolite horizon can be used as the Ordovician–Silurian boundary rather than the current assessed *Akidograptus ascensus* zone (Fig. 1b) (Berry, 1987). Additionally, the Ordovician–Silurian stratigraphic section from Anhui, China, is reported to have an ideal abundance and diversity of graptolites without tectonic disturbances making it an ideal candidate for the Ordovician–Silurian boundary GSSP (Ji-jin *et al.* 1984; Berry, 1987).

Due to Dob's Linn's SSSI status, it proved difficult to collect and obtain adequate sample sizes to generate the large quantities of zircon ideally used to produce robust ^{238}U – ^{206}Pb dates (Vermeesch, 2004; Andersen, 2005). However, with the samples provided, we were able to generate meaningful results. In addition, a comparison between LA-ICP-MS and CA-ID-TIMS results for the same grains

provides some important observations that should be made when assessing MDAs using the laser-based approach alone.

In the case of this study, the youngest chronostratigraphic sample is BRS23 from the *Coronagraptus cyphus* zone, presenting an LA-ICP-MS KDE distribution with a primary peak of 441 Ma showing a younger skewed tail incorporating Devonian zircon dates as young as 392 ± 10 Ma to as old as Ordovician 484 ± 13 Ma (Fig. 5a). The range of LA-ICP-MS dates from sample BRS23 are significantly younger and older than its currently recognized Silurian age of 439.57 ± 1.33 Ma (Tucker *et al.* 1990; Gradstein *et al.* 2020; Schmitz & Ogg, 2020), and this study's CA-ID-TIMS ^{238}U – ^{206}Pb WM date of 440.44 ± 0.72 Ma. The older CA-ID-TIMS dates from sample BRS23 confirm the presence of antecrysts with pre-eruptive growth in the zircon grains within this metabentonite (Wotzlaw *et al.* 2013; Schaltegger *et al.* 2014). As shown in Fig. 6, zircon grains with muted zoning textures have dates that are indicative of ash fall origins (autocrysts), and grains with oscillatory zoning as a result of episodic magmatic growths tend to be associated with antecrysts. The muted CL may reflect rapid crystallization of eruptive zircons from a single homogenous magma and could be useful in differentiating them from antecrysts. Due to detecting both autocrysts and antecrysts in this single bentonite layer at Dob's Linn, caution is necessary when dating this section with ID-TIMS multigrain zircon fractions without any zircon grain pre-screening by CL imaging or LA-ICP-MS.

Furthermore, it is important to note that most of the single-grain comparative dates between LA-ICP-MS and CA-ID-TIMS overlap within uncertainty except for the youngest and in some cases the oldest LA-ICP-MS dates (Fig. 7). For sample BRS23, Figs. 6 and 7 compares LA-ICP-MS and CA-ID-TIMS dates from the same individual grains where two of the youngest LA-ICP-MS population grains show differences of up to 40 Ma with CA-ID-TIMS showing Pb loss is present and effectively removed by the chemical abrasion treatment. In addition, LA-ICP-MS dates that are older than their CA-ID-TIMS dates (Figs 6 and 7; supplementary table S2) may reflect a mismatch in ablation rates between samples and standards that lead to bias in the U-Pb downhole fractionations. We refer to this matrix mismatch as it likely stems from different crystal lattice states of samples and standards. Although this effect can theoretically produce dates that are both too young and too old, standards are typically low in U and have less lattice damage than many samples, so the effect is skewed towards under-representation of U or apparent U loss and dates that are too old. The Concordia diagram in Fig. 8a used to evaluate the age consistency between the two chronometers ^{238}U – ^{206}Pb and ^{235}U – ^{207}Pb and disturbances within the U-Pb system by Pb loss displays a prominent age cluster. However, the BRS23 Concordia diagram also shows younger than expected clusters of LA-ICP-MS dates exhibiting Pb loss in the system. Using various LA-ICP-MS MDA calculation methods for sample BRS23, the YSG date of 392 ± 10 Ma (5% disc) and the YC2 σ +2 with a date of 397 ± 10 Ma ($n = 4$, MSWD = 1.40) produced the youngest MDA dates for this sample (Fig. 5a). The WM, MLA and TuffZirc date yielded dates of 439 ± 2 Ma ($n = 133$, MSWD = 5.60), 440 ± 2 Ma ($N = 133$, MSWD = 5.40) and $441+2/-3$ Ma ($n = 133$) overlapping within a larger uncertainty with the current interpreted age of 439.57 ± 1.33 Ma by Schmitz & Ogg (2020), and this study's CA-ID-TIMS ^{238}U – ^{206}Pb weighted mean date of $440.44 \pm 0.55/0.56/0.72$ Ma (\pm analytical/with tracer/with U-decay constant) (95% conf., MSWD 0.26, 4 of 15 analyses). However, the YMKDE with a date of 441 Ma and both the YSP and YMWM with the same date of 440 ± 1 Ma ($n = 83$, MSWD = 1.00) approximate the current

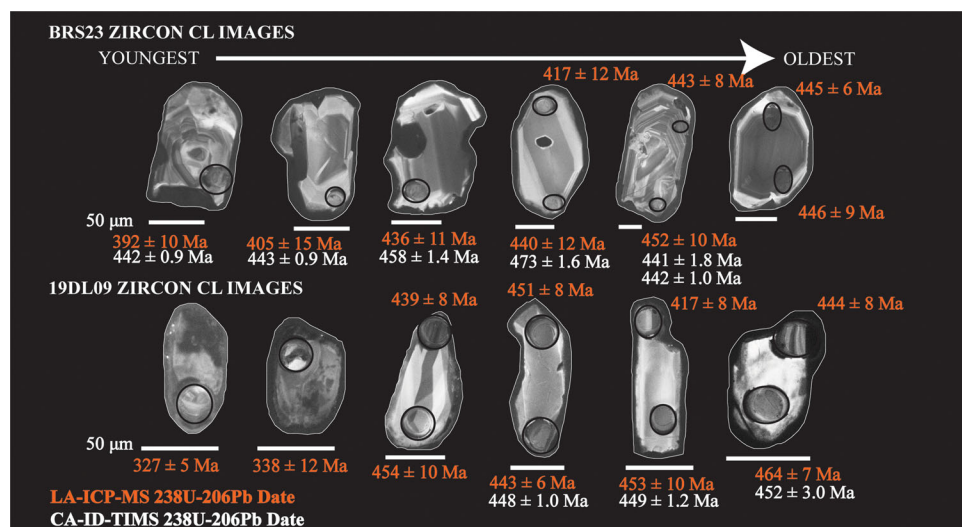


Figure 6. (Colour online) CL images of representative Dob's Linn metabentonite zircon grains with ^{238}U - ^{206}Pb LA-ICP-MS and CA-ID-TIMS dates. Ovals indicate locations of LA-ICP-MS analyses. Zircons with broad, muted zoning textures may reflect eruptive zircons, whereas tighter, concentric, oscillatory zoning is more typical of magmatic zircon growths. Bright cathodoluminescence zones correspond to high U content.

interpreted age of the biozone and our CA-ID-TIMS date with higher precision compared to the WM and Tuffzirc dates (Figs. 5a, and 9).

The *Akidograptus ascensus* zone associated with sample 19DL09 in this study is interpreted as the global standard reference section for the Ordovician–Silurian boundary with a calculated age of 443.8 ± 1.5 Ma with the use of spline fitting interpolation using various radioisotopic dates (Rong *et al.* 2008; Cohen *et al.* 2022). Sample 19DL09 in this study presents the first ^{238}U - ^{206}Pb zircon dates from a Dob's Linn metabentonite in the *Akidograptus ascensus* zone. The LA-ICP-MS KDE distribution shows two bimodal peaks, including Carboniferous zircon dates as young as 327 ± 5 Ma to as old as Ordovician 464 ± 7 Ma (Fig. 5b). Three significantly young Carboniferous zircon dates form the youngest peak shown in the KDE distribution. The second older peak comprises 14 zircon dates, from which most are Ordovician–Silurian age, except for one young Silurian–Devonian date. The range of LA-ICP-MS dates from sample 19DL09 is predominantly skewed towards significantly younger zircon dates than the current interpreted Ordovician–Silurian boundary age of 443.8 ± 1.5 Ma (Cohen *et al.* 2022). Using various LA-ICP-MS MDA calculation methods for sample 19DL09, the youngest MDA dates were produced with the YSG, YC2 σ +2, WM, YMKDE and YSP approaches (Fig. 5b). The YSG yielded a date of 327 ± 5 Ma (1% disc), and the YC2 σ +2 produced a date of 329 ± 13 ($n=3$, MSWD = 1.70). The WM yielded a date of 426 ± 22 Ma ($n=17$, MSWD = 134.00) and the MLA produced a date of 423 ± 23 Ma ($n=17$, MSWD = 110.00). The YMKDE shows a date of 331 Ma, and the YSP produced a date of 328 ± 5 ($n=2$, MSWD = 0.92). Only the TuffZirc date with a date of 447 ± 7 – 8 Ma ($n=13$) and the YMWM with a date of 441 ± 3 ($n=6$, MSWD = 0.96) calculated the current Ordovician–Silurian boundary age of 443.8 ± 1.5 Ma within uncertainty (Fig. 9).

Due to the destructive nature of the CA-ID-TIMS method, not all the youngest LA-ICP-MS dated zircon grains endure the chemical abrasion process, thus preventing this study from producing a robust ^{238}U - ^{206}Pb CA-ID-TIMS WM date for sample 19DL09. However, we present four individual CA-ID-TIMS zircon dates previously screened with LA-ICP-MS from a young and three older plateau population grains with ^{238}U - ^{206}Pb CA-ID-TIMS dates of 448.38 ± 1.10 Ma, 449.08 ± 1.20 Ma, 452.43 ± 3.00 Ma and 494.91 ± 1.40 Ma (supplementary table S2). As shown in Fig. 5, the

zircon grains from sample 19DL09 also display muted zoning textures reflecting ash fall origins (autocrysts) and oscillatory textured grain from previous magmatic growths (antecrysts) (Wotzlaw *et al.* 2013; Schaltegger *et al.* 2014). Two of the CA-ID-TIMS analyses, when compared to their respective LA-ICP-MS dates, yield slightly younger zircon dates with overlapping uncertainty (Fig. 7b). One grain shows a CA-ID-TIMS date slightly younger by 2 Ma than its LA-ICP-MS date (Figs. 6, and 7b). However, one anomalous grain from the youngest population of LA-ICP-MS dates produced a significantly older CA-ID-TIMS date by 160 Ma, yielding a CA-ID-TIMS date older than the stratigraphic age representing the inclusion of an inherited core based on its discordance (sample 19DL09 g2; Figs. 7b and 8b; supplementary table S2). The differences between the LA-ICP-MS and CA-ID-TIMS individual grain comparison for sample 19DL09 are interpreted to reflect both matrix mismatches and Pb loss effects for these zircon grains due to the younger and older dates when compared to CA-ID-TIMS dates. Concordia diagram in Fig. 8b illustrates two distinguishable clusters with the youngest cluster of LA-ICP-MS date manifesting significant Pb loss. The significant Pb loss effect is also reflected with the younger LA-ICP-MS younger zircon population (Fig. 5b). Furthermore, one grain from the youngest population of LA-ICP-MS dates with an anomalous Carboniferous young date of 338 ± 12 was not chemically abraded and dated with ID-TIMS yielding the same unusually young date of 339.64 ± 0.62 (supplementary table S2). These zircon dates yielding the same young dates support our interpretation that Pb loss is the dominant factor with the anomalously young grains dated using LA-ICP-MS and the chemical abrasion process is effective at removing the effects of Pb loss.

The oldest chronostratigraphic sample is DL7 from the *Dicellograptus anceps* zone showing a symmetric LA-ICP-MS KDE distribution with a single broad peak of 434 Ma incorporating Devonian zircon dates as young as 402 ± 12 Ma to as old as Ordovician 462 ± 10 Ma (Fig. 5c). The range of LA-ICP-MS dates from sample DL7 visually does not look skewed towards younger dates, but the majority of the grains yield predominantly younger zircon dates than its biozone's interpreted age of 444.88 ± 1.17 Ma (Gradstein *et al.* 2020; Schmitz & Ogg, 2020). Although we were unable to produce CA-ID-TIMS dates for sample DL7 due to loss of zircons to complete dissolution during the chemical abrasion

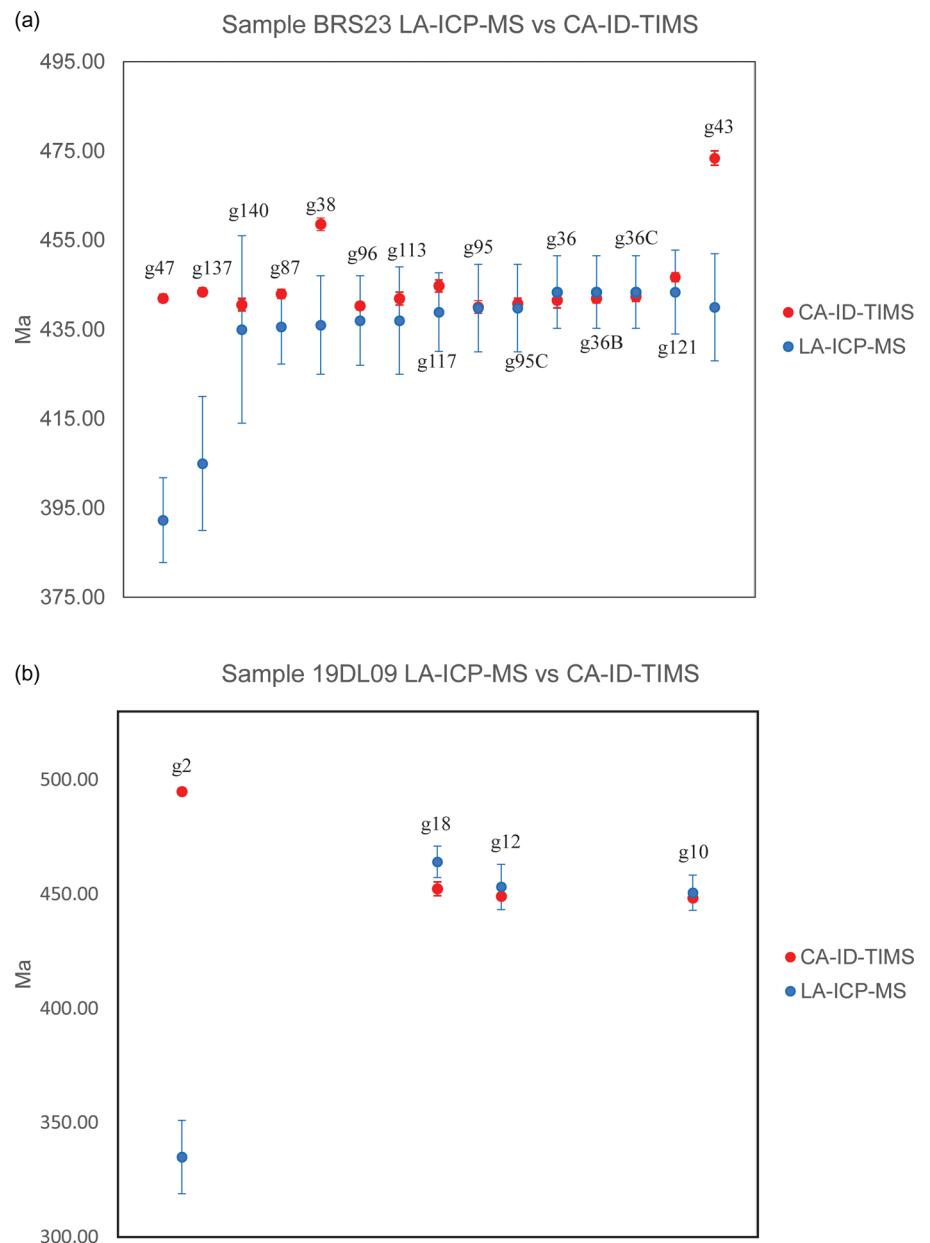


Figure 7. (Colour online) One-to-one comparison between individual LA-ICP-MS U-Pb (blue) vs. CA-ID-TIMS (red) U-Pb dates. Error bars represent 2σ uncertainty.

process, we present several LA-ICP-MS MDA calculation methods for the *Dicellograptus anceps* zone at Dob's Linn. The abundance of younger grains along with the complete dissolution of them is consistent with metamict zircons. All MDA approaches for sample DL7, including the YSG, YC2 σ +2, WM, TuffZirc date, MLA, YMKDE, YSP and YMWM, yielded significantly younger or inconsistent dates than the current assessed biozone age of 444.88 ± 1.17 Ma (Fig. 5c). The YSG yielded a date of 402 ± 12 Ma (5% disc), and the YC2 σ +2 produced a date of 423 ± 9 ($n = 4$, MSWD = 2.00). The WM yielded a date of 436 ± 4 Ma ($n = 26$, MSWD = 7.10), and the TuffZirc date produced a date of $435+5/-2$ Ma ($n = 25$). The MLA produces a date of 436 ± 5 Ma ($n = 26$, MSWD = 7.20). The YMKDE yielded a date of 434 Ma, and both the YSP and YMWM yielded the same date of 433 ± 2 ($n = 17$, MSWD = 1.00) (Figs. 5c, and 9). It is important to note that sample DL7, linked to the *Dicellograptus anceps* zone at Dob's Linn, comes from the Main Cliff locality rather than the Linn Branch GSSP location, only separated by several hundred metres horizontally

(Batchelor & Weir, 1988; Williams, 1988; Verniers & Vandembroucke, 2006). The Concordia diagram in Fig. 8c shows dispersed zircon dates including a minor cluster with large uncertainties approximating the current interpret age of 444.88 ± 1.17 Ma. However, a multitude of dates are significantly younger than expected manifesting significant Pb loss. The significant Pb loss effect is also reflected in the overall LA-ICP-MS KDE zircon distribution (Fig. 5c). Furthermore, one grain from the youngest population of LA-ICP-MS dates with an anomalous Carboniferous young date of 338 ± 12 was not chemically abraded and dated with ID-TIMS yielding the same unusual young date of 339.64 ± 0.62 (supplementary table S2). Based on the abundance of young LA-ICP-MS dates from sample DL7 showing younger MDA calculations than the youngest BRS23 sample in this study, the zircon grains in this particular horizon may have experienced more significant Pb loss, or the *Dicellograptus anceps* zone is incorrectly assigned in the Main Cliff locality (Fig. 9). As previously mentioned, the Dob's Linn locality is considerably tectonically and thermally disturbed where the same graptolite

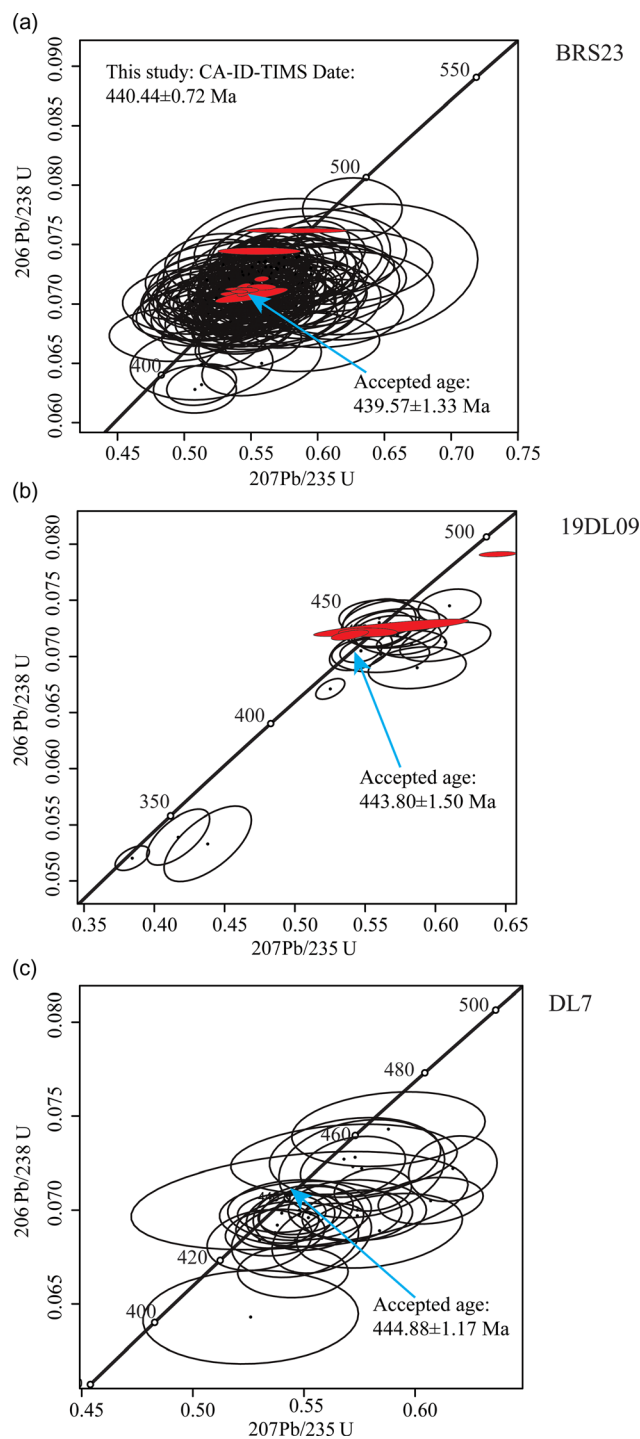


Figure 8. (Colour online) U-Pb LA-ICP-MS and CA-ID-TIMS Concordia diagram reported as total Pb for zircon data from metabentonites in the Hartfell and Birkhill shales at Dob's Linn, Scotland. (a) Sample BRS23: *Coronagraptus cyphus* zone, accepted age from Tucker *et al.* (1990). (b) Sample 19DL09: *Akidograptus ascensus* zone, accepted age from Cohen *et al.* (2022). (c) Sample DL7: *Dicellograptus anceps* zone, accepted age from Tucker *et al.* (1990). Black ovals show LA-ICP-MS dates, and red ovals display CA-ID-TIMS dates.

biozone identification occurs in different stratigraphic positions separated by large- and small-scale faults (Berry, 1987; Lesperance *et al.* 1987). Graptolite horizons in the Main Cliff locality can potentially be misplaced in the stratigraphy, thus not presenting the first appearance of a specific graptolite fauna but a later occurrence.

All three samples in this study demonstrate that MDA interpretations using YSG and YC2 σ +2 are invalid for this Early Paleozoic section. These approaches can be considered less conservative and follow the theory of using the youngest concordant zircons or youngest concordant zircon clusters as the maximum age of an enclosing sediment, thus often generating considerably younger dates than the true depositional age (TDA) (Herriott *et al.* 2019). As shown with this study's YSG and YC2 σ +2 dates, discordance alone is not adequate to identify Pb loss from Phanerozoic LA-ICP-MS data (Anderson *et al.* 2019). In all three samples (BRS23, 19DL09, DL7), the LA-ICP-MS YSG and YC2 σ +2 dates produced anomalous young dates (Fig. 5). For sample DL7, there are two possibilities (or possibly a combination) as to why we identify complications with the sample. The zircons experienced more Pb loss generating biases with the calculated MDA approaches or incorrect stratigraphic assignment. In the case of sample BRS23, the YSG and YC2 σ +2 yield much younger dates by 36 Ma and 31 Ma when compared with our CA-ID-TIMS date of 440.44 \pm 0.72 Ma and the current recognized *Coronagraptus cyphus* zone age of 439.57 \pm 1.33 Ma (Gradstein *et al.* 2020; Schmitz & Ogg, 2020). For sample 19DL09, the YSG and YC2 σ +2 yield significantly younger dates by 110 Ma and 100 Ma compared to the current recognized *Akidograptus ascensus* age of 443.8 \pm 1.5 Ma (Cohen *et al.* 2022). For sample DL7, the YSG and YC2 σ +2 yield younger dates by 30 Ma and 12 Ma compared to the current recognized *Dicellograptus anceps* age of 444.88 \pm 1.17 Ma (Gradstein *et al.* 2020; Schmitz & Ogg, 2020). The YMKDE yielded a suitable date of 441 Ma for sample BRS23 within uncertainty of its current assessed age. However, the YMKDE produced considerably younger dates of 110 Ma and 10 Ma for samples 19DL09 and DL7. The YSP approach only produced a suitable date for sample BRS23, comparable to this study's CA-ID-TIMS date and current recognized biozone age within uncertainty. However, the YSP yielded younger dates by 112 Ma and 9 Ma for samples 19DL09 and DL7. The TuffZirc date yielded appropriate dates for samples BRS23 and 19DL09, though with a considerably larger uncertainty when compared to our CA-ID-TIMS date or current recognized biozone age. In the case of sample DL7, the TuffZirc date provided a younger date by 4 Ma. Similarly, the YMWM also produced suitable dates for samples BRS23 and 19DL09 with improved uncertainty compared to the TuffZirc date, and within uncertainty of our CA-ID-TIMS date or current recognized biozone age. However, for sample DL7, the YMWM yields a date 9 Ma younger than its current assessed age.

The study's results suggest that both LA-ICP-MS and CA-ID-TIMS dating approaches are needed in localities like Dob's Linn, where extensive post-depositional structural and hydrothermal alterations produce a high percentage of discordant and potentially metamict zircons due to the widespread tectonic activity associated with the formation of the Caledonian mountains (Fig. 4) (Lesperance *et al.* 1987; Chew & Strachan, 2014). Integrating LA-ICP-MS and CA-ID-TIMS provides the benefit of pre-screening and eliminating possible older detrital grains and identifying target zircons from the youngest populations for CA-ID-TIMS analyses. The complex tectonic activity at Dob's Linn distorted the graptolite biozones in southern Scotland, inducing biostratigraphic misrepresentation and potentially influencing an increase in metamict grains, thus overall inducing younger U-Pb zircon dates due to Pb loss (Lesperance *et al.* 1987).

Comparative single grain dates between LA-ICP-MS and CA-ID-TIMS overlap within uncertainty predominantly with zircon plateau populations. However, this is not the case for the

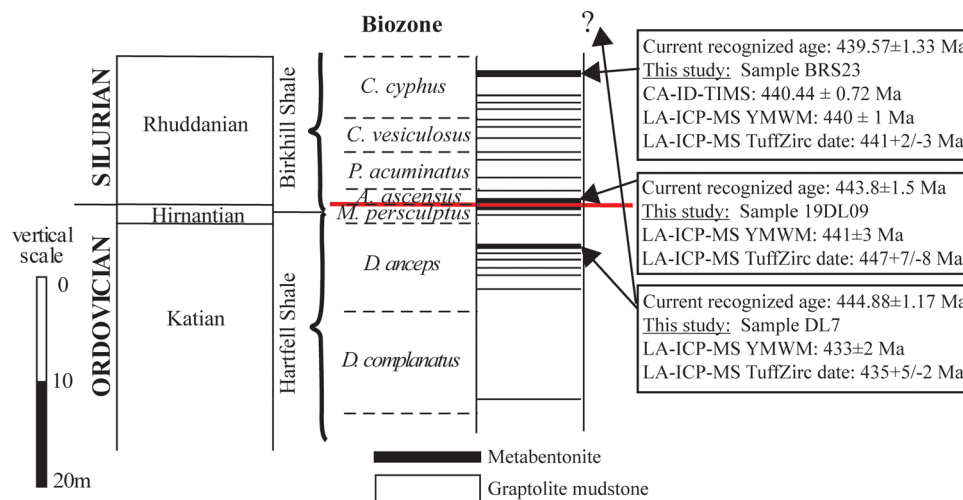


Figure 9. (Colour online) Hartfell and Birkhill Shale stratigraphy with graptolite biozones from Dob's Linn (after Batchelor & Weir, 1988; Merriman & Roberts, 1990). Samples BRS23 and 19DL09 from the Linn trench branch and DL7 from the Main cliff location. Comparison between currently recognized zone ages and new U-Pb dates presented in this study. *D. anceps* zone age from Tucker *et al.* (1990); *A. ascensus* zone age defining Ordovician–Silurian boundary (dashed line) from Cohen *et al.* (2022); *C. cyphus* zone age from Tucker *et al.* (1990). LA-ICP-MS YMW and TuffZirc date MDA approaches present suitable dates for samples BRS23 and 19DL09 to currently recognized biozone ages, and this study's BRS23 CA-ID-TIMS date. Sample DL7 displays potential stratigraphic misplacement or significant Pb loss presented by the younger MDA dates than sample BRS23.

youngest individual grains and clusters with differences of more than 100 Ma due to Pb loss and matrix mismatch influence. Additionally, individual LA-ICP-MS dates that are older than CA-ID-TIMS dates are interpreted to reflect a matrix mismatch that biases the U-Pb downhole fractionation (Figs. 5, and 7, supplementary table S2). The best LA-ICP-MS MDA estimates are generated from calculations using averages and not primarily the youngest grains so that both Pb loss and matrix mismatch effects are minimized (e.g., Tian *et al.* 2022). In cases where significant number of zircons have experienced Pb loss, the chemical abrasion process becomes crucial, as averages may not provide accurate results. Our study's findings support the conclusions of Tian *et al.* (2022) with the TuffZirc date and YMW yielded the best results to achieve appropriate MDAs estimation when only LA-ICP-MS data is available. For this study, the LA-ICP-MS MDA methodologies such as the TuffZirc date and YMW yielded results that were in line with CA-ID-TIMS analysis, within the margin of uncertainty. This outcome was achieved by employing average calculations that encompassed both the youngest grains affected by variable Pb loss and moderately older grains that remained unaffected by significant Pb loss. The TuffZirc date by Ludwig and Mundil (2002) demonstrated suitable results, although with larger uncertainty for two of our three samples, and generated a young MDA for the third complex sample (DL7) by only 4 Ma younger than its current assessed age (Fig. 9). The YMW from Tian *et al.* (2022) also generated appropriate results, though more robust with superior uncertainty than the TuffZirc date for two of our three samples; however, for the third problematic sample (DL7), the approach determined an MDA date 9 Ma younger than its current assessed age (Fig. 9). The TuffZirc date and YMW present younger dates for the older *Dicellograptus anceps* zone (sample DL7) than the current recognized age and our CA-ID-TIMS date for the *Coronagraptus cyphus* zone (sample BRS23), which is considered the youngest stratigraphic sample in this study.

Based on the GSSP requirements by the ICS, including the findings from previous studies describing the inconsistencies of Dob's Linn as a reference section, and our finding in this study, such as the potential of the *Dicellograptus anceps* zone being incorrectly

assigned stratigraphically, Dob's Linn's GSSP status appears to be questionable (Berry, 1987; Lesperance *et al.* 1987; Remane *et al.* 1996). We suggest the re-examination of Dob's Linn, both with biostratigraphy and additional sample collection for future CA-ID-TIMS zircon dates to improve accuracy and precision or considering other Ordovician–Silurian boundary outcrops such as the ones in Anticosti Island, Canada or South China for future studies involving the Ordovician–Silurian periods.

8. Conclusions

This study presents new data from the *Dicellograptus anceps*, *Akidograptus ascensus* and *Coronagraptus cyphus* zones at Dob's Linn, Scotland. We produced a high-precision CA-ID-TIMS date of $440.44 \pm 0.55/0.56/0.72$ Ma (\pm analytical/with tracer/with U-decay constant) for the *Coronagraptus cyphus* zone. Comparisons between CA-ID-TIMS and LA-ICP-MS U-Pb zircon dates for the metabentonites encompassing the *Akidograptus ascensus* and *Coronagraptus cyphus* zones demonstrate the presence of both autocrysts and antecrysts in addition to significant Pb loss and matrix mismatch between LA-ICP-MS unknowns and standards (Figs. 5–7; supplementary table S2). The presence of autocrysts and antecrysts in Dob's Linn holds significance due to its impact on the accuracy of the established biozone ages. Previously, these ages were determined with multigrain zircon fractions ID-TIMS analyses (Tucker *et al.* 1990). Comparative single U-Pb dates between LA-ICP-MS and CA-ID-TIMS overlap within uncertainty primarily with zircon plateau populations; however, this is not the case for the youngest grains and youngest cluster populations showing anomalous differences of more than 100 Ma with the currently assessed biozone ages and our CA-ID-TIMS dates (supplementary table S2). The Pb loss and matrix mismatch is corroborated with the notably younger zircon dates and older individual LA-ICP-MS dates compared to individual CA-ID-TIMS analyses (Figs. 6 and 7; supplementary table S2).

We suggest integrating LA-ICP-MS and CA-ID-TIMS whenever possible for MDA calculations to screen and eliminate older detrital grains and focus on the youngest individual grains and

populations for CA-ID-TIMS analyses. In cases where CA-ID-TIMS analysis is not feasible, we strongly advocate the annealing of both unknown and standard zircon grains to enhance and standardize matrix conditions (Allen & Campbell, 2012). MDAs based on a small number of grains (i.e., YSG, YC2 σ +2) are unreliable in our study. We recommend utilizing MDA calculations by considering averages of grains beyond solely relying on the youngest zircon grains to mitigate potential issues related to Pb loss and matrix mismatch effects. MDA methodologies such as the TuffZirc date and YMWM demonstrated optimal performance attributed to the incorporation of older co-genetic LA-ICP-MS zircon dates that remained unaffected by substantial Pb loss. As a result, these older co-genetic dates superseded the influence of younger grains impacted by variations of Pb loss. Based on our results, the TuffZirc date and YMWM produced adequate MDA calculations when only LA-ICP-MS data is available as they yield comparable results to our CA-ID-TIMS analyses or the currently recognized biozone ages within uncertainty (Fig. 9) (Ludwig & Mundil, 2002; Tian *et al.* 2022). In the case of sample DL7, we are uncertain whether sample DL7 associated with the *Dicellograptus anceps* zone at Dob's Linn reflect Pb loss, stratigraphic misplacement, or both due to widespread tectonic and thermal activity. More sample material from the Dob's Linn locality is necessary to acquire additional CA-ID-TIMS analyses. The LA-ICP-MS TuffZirc date and YMWM MDA approaches indicate younger dates for the *Dicellograptus anceps* zone than the youngest sample of the study BRS23 from the *Coronagraptus cyphus* zone (Fig. 9). The potential biostratigraphy and stratigraphic misplacement encountered with this study, along with the International Commission of Stratigraphy (ICS) GSSP requirements and previous reports of the inadequacy of Dob's Linn as a global reference section, raises concerns on the validity of Dob's Linn as the Ordovician–Silurian GSSP type section (Berry, 1987; Lesperance *et al.* 1987; Remane *et al.* 1996). A comprehensive future re-examination of Dob's Linn is essential using biostratigraphy and geochronology to assess the legitimacy of Dob's Linn as a GSSP and the appointment of a new proper location as the Ordovician–Silurian boundary GSSP.

Supplementary material. To view supplementary material for this article, please visit <https://doi.org/10.1017/S0016756823000717>

Acknowledgements. Data supporting the conclusions can be obtained from the supplementary material (supplementary tables S1 and S2) and will be placed in the Cambridge University Press Supplementary Material data archive and the British Geological Survey database repository. We appreciate funding for this work by the National Science Foundation/Geological Society of America Graduate Student Geoscience Grant #13555-22, which is funded by NSF Award # 1949901, and a Student Research Award from the University of Texas at Austin (UT Austin) Center for Planetary Systems Habitability. Support funds were also attained by E.J. Catlos (UT Austin's Jackson School of Geosciences (JSG) Centennial Teaching Fellowship and the Faculty Innovation Center. U-Pb dates were collected at the JSG UTChron Laboratory at UT Austin and at the U-Pb Geochronology Laboratory in the Department of Geology and Geophysics at the University of Wyoming. We appreciate analytical assistance by L. Stockli and comments from J. Clarke, M. Malkowski, and S. Loewy (Department of Geological Sciences, UT Austin). We appreciate comments from one anonymous reviewer and G. Sharman. We appreciate samples provided by S.F. Parry at the British Geological Survey, Environmental Science Centre and acknowledge J. Kerr from NatureScot, for permission to responsibly sample Dob's Linn.

Competing interests. The author(s) declare none.

References

- Agterberg FP, DaSilva AC and Gradstein FM (2020) Geomathematical and statistical procedures. In *Geologic Time Scale 2020* (eds FM Gradstein, JG Ogg, MD Schmitz, and GM Ogg), 2, pp. 402–525. Amsterdam, Netherlands: Elsevier. Print.
- Allen CM and Campbell IH (2012) Identification and elimination of a matrix-induced systematic error in LA-ICP-MS ²⁰⁶Pb/²³⁸U dating of zircon. *Chemical Geology* **332**, 157–65.
- Andersen T (2005) Detrital zircons as tracers of sedimentary provenance: limiting conditions from statistics and numerical simulation. *Chemical Geology* **216**, 249–70.
- Andersen T, Elburg MA and Magwaza BN (2019) Sources of bias in detrital zircon geochronology: discordance, concealed lead loss and common lead correction. *Earth-Science Reviews* **197**, 1–15.
- Anderson HS, Yoshinobu AS, Nordgulen Ø and Chamberlain K (2013) Batholith tectonics: formation and deformation of ghost stratigraphy during assembly of the mid-crustal Andalshatten batholith, central Norway. *Geosphere* **9**, 667–90.
- Balan E, Trocellier P, Jupille J, Fritsch E, Muller JP and Calas G (2001) Surface chemistry of weathered zircons. *Chemical Geology* **181**, 13–22.
- Barnes CG, Coint N, Barnes MA, Chamberlain KR, Cottle JM, Rämö OT, Strickland A and Valley JW (2021) Open-system evolution of a crustal-scale magma column, Klamath mountains, California. *Journal of Petrology* **62**, 1–29.
- Bassett MG (1985) Towards a “common language” in stratigraphy. *Episodes Journal of International Geoscience* **8**, 87–92.
- Batchelor RA and Weir JA (1988) Metabentonite geochemistry: magmatic cycles and graptolite extinctions at Dob's Linn, southern Scotland. *Earth and Environmental Science Transactions of the Royal Society of Edinburgh* **79**, 19–41.
- Berry WB (1987) The Ordovician–Silurian boundary: new data, new concerns. *Lethaia* **20**, 209–16.
- Bowring SA and Schmitz MD (2003) High-precision U-Pb zircon geochronology and the stratigraphic record. *Reviews in Mineralogy and Geochemistry* **53**, 305–26.
- Bowring SA, Schoene B, Crowley JL, Ramezani J and Condon DJ (2006) High-precision U-Pb zircon geochronology and the stratigraphic record: progress and promise. *The Paleontological Society Papers* **12**, 25–45.
- Brookfield ME, Catlos EJ and Suarez SE (2021) Myriapod divergence times differ between molecular clock and fossil evidence: U/Pb zircon ages of the earliest fossil millipede-bearing sediments and their significance. *Historical Biology* **33**, 2009–13.
- Carroll D (1953) Weatherability of zircon. *Journal of Sedimentary Research* **23**, 106–16.
- Carruthers W (1858) Dumfriesshire graptolites, with descriptions of three new species. In *Proceedings of the Royal physical Society of Edinburgh* **1**, 466–70.
- Catlos EJ, Mark DF, Suarez S, Brookfield ME, Miller CG, Schmitt AK, Gallagher V and Kelly A (2021) Late Silurian zircon U-Pb ages from the Ludlow and Downton bone beds, Welsh Basin, UK. *Journal of the Geological Society* **178**, 1–18.
- Chew DM and Strachan RA (2014) The Laurentian Caledonides of Scotland and Ireland. *Geological Society, London, Special Publications* **390**, 45–91.
- Cocks LRM (1985) The Ordovician–Silurian boundary. *Episodes Journal of International Geoscience* **8**, 98–100.
- Cocks LRM (1988) The Ordovician–Silurian boundary and its working group. *Bulletin of the British Museum (Natural History)* **43**, 9.
- Cohen KM, Finney SC, Gibbard PL and Fan J-X (2013) The ICS International Chronostratigraphic Chart. *Episodes Journal of International Geoscience* **36**, 199–204.
- Cohen KM, Harper DAT and Gibbard PL (2022) ICS International Chronostratigraphic Chart 2022/10. International Commission on Stratigraphy, IUGS. www.stratigraphy.org
- Condon DJ and Bowring SA (2011) A user's guide to Neoproterozoic geochronology. *Geological Society, London, Memoirs* **36**, 135–49.
- Corfu F (2013) A century of U-Pb geochronology: the long quest towards concordance. *GSA Bulletin* **125**, 33–47.

- Coutts DS, Matthews WA and Hubbard SM** (2019) Assessment of widely used methods to derive depositional ages from detrital zircon populations. *Geoscience Frontiers* **10**, 1421–35.
- Crowley QG, Heron K, Riggs N, Kamber B, Chew D, McConnell B and Benn K** (2014) Chemical abrasion applied to LA-ICP-MS U–Pb zircon geochronology. *Minerals* **4**, 503–18.
- Dahl TW, Hammarlund EU, Rasmussen CMØ, Bond DP and Canfield DE** (2021) Sulfidic anoxia in the oceans during the Late Ordovician mass extinctions—insights from molybdenum and uranium isotopic global redox proxies. *Earth-Science Reviews* **220**, 1–14.
- Dickinson WR and Gehrels GE** (2009) Use of U–Pb ages of detrital zircons to infer maximum depositional ages of strata: a test against a Colorado Plateau Mesozoic database. *Earth and Planetary Science Letters* **288**, 115–25.
- Finch RJ and Hanchar JM** (2003) Structure and chemistry of zircon and zircon-group minerals. *Reviews in Mineralogy and Geochemistry* **53**, 1–25.
- Finney S** (2005) Global series and stages for the Ordovician system: a progress report. *Geologica Acta* **3**, 309–16.
- Finney S and Chen X** (1990) The relationship of Ordovician graptolite provincialism to palaeogeography. *Geological Society, London, Memoirs* **12**, 123–8.
- Fortey RA** (2011) A critical graptolite correlation into the Lower Ordovician of Gondwana. *Proceedings of the Yorkshire Geological Society* **58**, 223–6.
- Frei D and Gerdes A** (2009) Precise and accurate in situ U–Pb dating of zircon with high sample throughput by automated LA-SF-ICP-MS. *Chemical Geology* **261**, 261–70.
- Gradstein F, Ogg JG, Schmitz MD and Ogg GM** (2012) *The Geologic Time Scale 2012*. (1st ed.). San Diego: Elsevier, Print.
- Gradstein FM and Ogg JG** (2020) The chronostratigraphic scale. In *Geologic Time Scale 2020* (eds FM Gradstein, JG Ogg, MD Schmitz and GM Ogg), pp. 21–32. Amsterdam, Netherlands: Elsevier, Print.
- Gradstein FM, Ogg JG, Schmitz MD and Ogg GM** (Eds.). (2020) *Geologic Time Scale 2020*. Amsterdam, Netherlands: Elsevier, Print. 631–732.
- Herrriott TM, Crowley JL, Schmitz MD, Wartes MA and Gillis RJ** (2019) Exploring the law of detrital zircon: LA-ICP-MS and CA-TIMS geochronology of Jurassic forearc strata, Cook Inlet, Alaska, USA. *Geology* **47**, 1044–8.
- Holmes A** (1911) The association of lead with uranium in rock-minerals, and its application to the measurement of geological time. *Proceedings of the Royal Society of London. Series A, Containing Papers of a Mathematical and Physical Character* **85**, 248–56.
- Hu Y, Zhou J, Song B, Li W and Sun W** (2008) SHRIMP zircon U–Pb dating from K-bentonite in the top of Ordovician of Wangjiawan Section, Yichang, Hubei, China. *Science in China Series D: Earth Sciences* **51**, 493–8.
- Huff WD, Bergström SM and Kolata DR** (2010) Ordovician explosive volcanism. *The Ordovician Earth System* **466**, 13–28.
- Jackson SE, Pearson NJ, Griffin WL and Belousova A** (2004) The application of laser ablation-inductively coupled plasma-mass spectrometry to in situ U–Pb zircon geochronology. *Chemical Geology* **211**, 47–69.
- Ji-Jin L, Yi-Yuan Q and Jun-Ming Z** (1984) Ordovician–Silurian boundary section from Jiangxian, South Anhui. In *Stratigraphy and Palaeontology of Systemic Boundaries in China: Ordovician–Silurian Boundary* (ed Mu en-zhi), pp. 309–370. Compiled by Nanjing Institute of Geology and Palaeontology, Academia Sinica. Anhui Science and Technology Publishing House.
- Koren TN and Rickards RB** (1979) Extinction of the graptolites. *Geological Society, London, Special Publications* **8**, 457–466.
- Krogh TE** (1973) A low-contamination method for hydrothermal decomposition of zircon and extraction of U and Pb for isotopic age determinations. *Geochimica et Cosmochimica Acta* **37**, 485–94.
- Kunk MJ, Sutter J, Obradovich JD and Lanphere MA** (1985) Age of biostratigraphic horizons within the Ordovician and Silurian systems. *The Chronology of the Geological Record Geological Society, London, Memoir* **10**, 89–92.
- Lanphere MA, Churkin M and Eberlein GD** (1977) Radiometric age of the Monograptus cyphus graptolite zone in Southeastern Alaska—an estimate of the age of the Ordovician–Silurian boundary. *Geological Magazine* **114**, 15–24.
- Lapworth C** (1878) The Moffat series. *Quarterly Journal of the Geological Society* **34**, 240–346.
- Leggett JK, McKerrow WT and Eales MH** (1979) The Southern Uplands of Scotland: a lower Palaeozoic accretionary prism. *Journal of the Geological Society* **136**, 755–70.
- Lenton TM, Crouch M, Johnson M, Pires N and Dolan L** (2012) First plants cooled the Ordovician. *Nature Geoscience* **5**, 86–9.
- Lesperance PJ, Barnes CR, Berry WB, Boucot AJ and En-Zhi M** (1987) The Ordovician–Silurian boundary stratotype: consequences of its approval by the IUGS. *Lethaia* **20**, 217–22.
- Ling MX, Zhan RB, Wang GX, Wang Y, Amelin Y, Tang P, Liu JB, Jin J, Huang B, Wu RC, Xue S, Fu B, Bennett VC, Wei X, Luan XC, Finnegan S, Harper DAT and Rong JY** (2019) An extremely brief end Ordovician mass extinction linked to abrupt onset of glaciation. *Solid Earth Sciences* **4**, 190–8.
- Ludwig KR** (2008) Isoplot version 4.15: a geochronological toolkit for Microsoft Excel. *Berkeley Geochronology Center, Special Publication* **4**, 247–70.
- Ludwig KR and Mundil R** (2002) Extracting reliable U–Pb ages and errors from complex populations of zircons from Phanerozoic tuffs. *Geochimica et Cosmochimica Acta* **66**, 463.
- Mako CA, Law RD, Caddick MJ, Kylander-Clark A, Thigpen JR, Ashley KT, Mazza SE and Cottle J** (2021) Growth and fluid-assisted alteration of accessory phases before, during and after Rodinia breakup: U–Pb geochronology from the Moine Supergroup rocks of northern Scotland. *Precambrian Research* **355**, 1–21.
- Marillo-Sialer E, Woodhead J, Hergt J, Greig A, Guillion M, Gleadow A, Evans N and Paton C** (2014) The zircon ‘matrix effect’: evidence for an ablation rate control on the accuracy of U–Pb age determinations by LA-ICP-MS. *Journal of Analytical Atomic Spectrometry* **29**, 981–9.
- Marsh JH and Stockli DF** (2015) Zircon U–Pb and trace element zoning characteristics in an anatectic granulite domain: Insights from LASS-ICP-MS depth profiling. *Lithos* **239**, 170–85.
- Mattinson JM** (2005) Zircon U–Pb chemical abrasion (“CA-TIMS”) method: combined annealing and multi-step partial dissolution analysis for improved precision and accuracy of zircon ages. *Chemical Geology* **220**, 47–66.
- Mattinson JM** (2013) Revolution and evolution: 100 years of U–Pb geochronology. *Elements* **9**, 53–7.
- Merriman RJ and Roberts B** (1990) Metabentonites in the Moffat Shale Group, Southern Uplands of Scotland: geochemical evidence of Ensialic marginal basin volcanism. *Geological Magazine* **127**, 259–71.
- Morris JH** (1987) The northern belt of the Longford-Down Inlier, Ireland and Southern Uplands, Scotland: an Ordovician back-arc basin. *Journal of the Geological Society* **144**, 773–86.
- Nicholson HA** (1867) Graptolites of the Moffat Shales. *Geological Magazine* **4**, 135–6.
- Ogg JG, Ogg GM and Gradstein FM** (2016) *A Concise Geologic Time Scale: 2016*. Amsterdam, Netherlands: Elsevier, Print. 57–84.
- Pogson DJ** (2009) The Siluro-Devonian geological time scale: a critical review and interim revision. *Quarterly Notes of the Geological Survey of New South Wales* **130**, 1–13.
- Rasmussen C, Stockli DF, Ross CH, Pickersgill A, Gulick SP, Schmieder M, Christeson G, Wittmann A, Kring DA, Morgan JV and Party S** (2019) U–Pb memory behavior in Chicxulub’s peak ring—applying U–Pb depth profiling to shocked zircon. *Chemical Geology* **525**, 356–67.
- Remane J, Bassett MG, Cowie JW, Gohrbandt KH, Lane HR, Michelsen O and Naiwen W** (1996) Revised guidelines for the establishment of global chronostratigraphic standards by the International Commission on Stratigraphy (ICS). *Episodes Journal of International Geoscience* **19**, 77–81.
- Rong J, Melchin M, Williams SH, Koren TN and Verniers J** (2008) Report of the restudy of the defined global stratotype of the base of the Silurian system. *Episodes Journal of International Geoscience* **31**, 315–8.
- Ross JB, Ludvigson GA, Möller A, Gonzalez LA and Walker JD** (2017) Stable isotope paleohydrology and chemostratigraphy of the Albian Wayan formation from the wedge-top depozone, North American Western Interior Basin. *Science China Earth Sciences* **60**, 44–57.
- Ross Jr RJ** (1984) The Ordovician system, progress and problems. *Annual Review of Earth and Planetary Sciences* **12**, 307–35.

- Ross RJ, Naeser CW, Izett GA, Obradovich JD, Bassett MG, Hughes CP, Cocks LRM, Dean WT, Ingham JK, Jenkins CJ, Rickards RB, Sheldon PR, Toghiani P, Whittington HB and Zalasiewicz J (1982) Fission-track dating of British Ordovician and Silurian stratotypes. *Geological Magazine* **119**, 135–53.
- Rosignol C, Hallot E, Bourquin S, Poujol M, Jolivet M, Pellenard P, Ducassou C, Nalpas T, Heilbronn G, Yu J and Dabard MP (2019) Using volcanoclastic rocks to constrain sedimentation ages: to what extent are volcanism and sedimentation synchronous?. *Sedimentary Geology* **381**, 46–64.
- Schaltegger U, Schmitt AK and Horstwood MSA (2015) U–Th–Pb zircon geochronology by ID-TIMS, SIMS, and laser ablation ICP-MS: recipes, interpretations, and opportunities. *Chemical Geology* **402**, 89–110.
- Schaltegger U, Wotzlaw JF, Ovtcharova M, Chiaradia M and Spikings R (2014) Mass spectrometry in Earth sciences: the precise and accurate measurement of time. *Chimia* **68**, 124.
- Schmitz MD and Ogg GM (2012) Appendix 2—Radiometric ages used in GTS2012. In *The Geologic Time Scale 2012* (eds, FM Gradstein, JG Ogg, MD Schmitz, and GM Ogg), pp. 1045–82. Amsterdam, Netherlands: Elsevier, Print.
- Schmitz MD and Ogg GM (2020) Appendix 2—Radiometric ages used in GTS2020. In *The Geologic Time Scale 2020* (eds, FM Gradstein, JG Ogg, MD Schmitz, and GM Ogg), pp. 1285–341. Amsterdam, Netherlands: Elsevier, Print.
- Schoene B (2014) 4.10-U–Th–Pb geochronology. *Treatise on Geochemistry* **4**, 341–78.
- Schoene B, Condon DJ, Morgan L and McLean N (2013) Precision and accuracy in geochronology. *Elements* **9**, 19–24.
- Servais T, Cascales-Miñana B, Cleal CJ, Gerrienne P, Harper DA and Neumann M (2019) Revisiting the Great Ordovician Diversification of land plants: recent data and perspectives. *Palaeogeography, Palaeoclimatology, Palaeoecology* **534**, 1–13.
- Sharman GR and Malkowski MA (2020) Needles in a haystack: Detrital zircon UPb ages and the maximum depositional age of modern global sediment. *Earth-Science Reviews* **203**, 1–23.
- Sharman GR, Sharman JP and Sylvester Z (2018) detritalPy: a Python-based toolset for visualizing and analysing detrital geo-thermochronologic data. *The Depositional Record* **4**, 202–15.
- Sláma J, Košler J, Condon DJ, Crowley JL, Gerdes A, Hanchar JM, Horstwood MSA, Morris GA, Nasdala L, Norberg N, Schaltegger U, Schoene B, Tubrett MN and Whitehouse MJ (2008) Plešovice zircon—a new natural reference material for U–Pb and Hf isotopic microanalysis. *Chemical Geology* **249**, 1–35.
- Solari LA, Ortega-Obregón C and Bernal JP (2015) U–Pb zircon geochronology by LAICPMS combined with thermal annealing: achievements in precision and accuracy on dating standard and unknown samples. *Chemical Geology* **414**, 109–23.
- Spencer CJ, Kirkland CL and Taylor RJ (2016) Strategies towards statistically robust interpretations of in situ U–Pb zircon geochronology. *Geoscience Frontiers* **7**, 581–9.
- Stone P, Floyd JD, Barnes RP and Lintern BC (1987) A sequential back-arc and foreland basin thrust duplex model for the Southern Uplands of Scotland. *Journal of the Geological Society* **144**, 753–64.
- Sweet WC and Bergström SM (1984) Conodont provinces and biofacies of the Late Ordovician. *Geological Society of America Special Paper* **196**, 69–87.
- Tian H, Fan M, Victor V, Chamberlain K, Waite L, Stern RJ and Loocke M (2022) Rapid early Permian tectonic reorganization of Laurentia's plate margins: evidence from volcanic tuffs in the Permian Basin, USA. *Gondwana Research* **111**, 76–94.
- Tichomirowa M, Kässner A, Sperner B, Lapp M, Leonhardt D, Linnemann U, Munker C, Ovtcharova M, Pfander JA, Schaltegger U, Sergeev S, von Quadt A and Whitehouse M (2019) Dating multiply overprinted granites: the effect of protracted magmatism and fluid flow on dating systems (zircon U–Pb: SHRIMP/SIMS, LA-ICP-MS, CA-ID-TIMS; and Rb–Sr, Ar–Ar)–Granites from the Western Erzgebirge (Bohemian Massif, Germany). *Chemical Geology* **519**, 11–38.
- Tucker RD, Krogh TE, Ross Jr RJ and Williams SH (1990) Time-scale calibration by high-precision UPb zircon dating of interstratified volcanic ashes in the Ordovician and Lower Silurian stratotypes of Britain. *Earth and Planetary Science Letters* **100**, 51–8.
- Ver Hoeve TJ, Scoates JS, Wall CJ, Weis D and Amini M (2018) Evaluating downhole fractionation corrections in LA-ICP-MS U–Pb zircon geochronology. *Chemical Geology* **483**, 201–17.
- Vermeesch P (2004) How many grains are needed for a provenance study? *Earth and Planetary Science Letters* **224**, 441–51.
- Vermeesch P (2012) On the visualization of detrital age distributions. *Chemical Geology* **312**, 190–4.
- Vermeesch P (2018) IsoplotR: a free and open toolbox for geochronology. *Geoscience Frontiers* **9**, 1479–93.
- Vermeesch P (2021) Maximum depositional age estimation revisited. *Geoscience Frontiers* **12**, 843–50.
- Verniers J and Vandembroucke TR (2006) Chitinozoan biostratigraphy in the Dob's Linn Ordovician–Silurian GSSP, Southern Uplands, Scotland. *GFF* **128**, 195–202.
- Von Quadt A, Gallhofer D, Guillong M, Peytcheva I, Waelle M and Sakata S (2014) U–Pb dating of CA/non-CA treated zircons obtained by LA-ICP-MS and CA-TIMS techniques: impact for their geological interpretation. *Journal of Analytical Atomic Spectrometry* **29**, 1618–29.
- Wallace MW, Shuster A, Greig A, Planavsky NJ and Reed CP (2017) Oxygenation history of the Neoproterozoic to early Phanerozoic and the rise of land plants. *Earth and Planetary Science Letters*, **466**, 12–9.
- Watts KE, Coble MA, Vazquez JA, Henry CD, Colgan JP and John DA (2016) Chemical abrasion-SIMS (CA-SIMS) U–Pb dating of zircon from the late Eocene Caetano caldera, Nevada. *Chemical Geology* **439**, 139–51.
- Williams SH (1983) The Ordovician–Silurian boundary graptolite fauna of Dob's Linn, southern Scotland. *Palaeontology* **26**, 605–39.
- Williams SH (1988) Dob's Linn—the Ordovician–Silurian Boundary. *Bulletin of the British Museum (Natural History)* **43**, 17–30.
- Williams SH and Rickards RB (1984) Palaeoecology of graptolitic black shales. In : *Aspects of the Ordovician System* (ed DL Bruton), **295**, pp. 159–66. Oslo: Universitetsforlaget, Print. Paleontological Contributions from the University of Oslo.
- Wotzlaw JF, Schaltegger U, Frick DA, Dungan MA, Gerdes A and Günther D (2013). Tracking the evolution of large-volume silicic magma reservoirs from assembly to supereruption. *Geology* **41**, 867–70.
- Zalasiewicz J (2001) Graptolites as constraints on models of sedimentation across Iapetus: a review. *Proceedings of the Geologists' Association* **112**, 237–51.
- Zellmer GF (2021) Gaining acuity on crystal terminology in volcanic rocks. *Bulletin of Volcanology* **83**, 78.
- Zhang X, Pease V, Skogseid J and Wohlgenuth-Ueberwasser C (2016) Reconstruction of tectonic events on the northern Eurasia margin of the Arctic, from U–Pb detrital zircon provenance investigations of late Paleozoic to Mesozoic sandstones in southern Taimyr Peninsula. *Geological Society of America Bulletin* **128**, 29–46.